Optimisation of Photonic Crystal Waveguide based Optical Filter

A Thesis submitted to the
Dept. of Electrical & Electronic Engineering, BRAC University
in partial fulfilment of the requirements for the
Bachelor of Science degree in Electrical & Electronic Engineering

PRATIK AL ISLAM

NAMEEZA SULTAN

SEEFATH NAYEEM

April 2013

Declaration

We do hereby declare that the thesis titled "Optimisation of Photonic Crystal waveguide based Optical Filter" is submitted to the Department of Electrical and Electronics Engineering of BRAC University in partial fulfillment of the Bachelor of Science in Electrical and Electronics Engineering. This is our original work and was not submitted elsewhere for the award of any other degree or any other publication.

Date:

Dr. Md. Belal Hossain Bhuian
Thesis Supervisor

_____

_____
Pratik Al Islam
Student ID: 10121015

_____
Nameeza Sultan
Student ID: 10121016

_____
Seefath Nayeem
Student ID: 10121020

ACKNOWLEDGEMENT

We are extremely grateful to our supervisor, Asst. Prof. Dr. Md. Belal Hossain Bhuian, for his guidance and discussions. Without his continuous support this thesis would not have been possible.

ABSTRACT

Photonic integrated circuits (PIC) based on Photonic Crystals are becoming increasingly favoured in emerging signal processing and optical communication technologies. Photonic crystals (PhCs) are periodic dielectric micro/nano structures that inhibit propagation of electromagnetic wave of a certain range of frequencies, therefore introducing a frequency band gap, popularly known as photonic band gap. In this thesis, numerical simulation of a photonic crystal based optical filter or demultiplexer is carried out by the introduction of defect rods in a perfectly periodic photonic crystal, whose parameters are chosen using the band gap map. The dimensions of the defect rods are exclusively tailored for the wavelength to be extracted via that channel. Optimisation of the proposed design by changing the number of rods in the defects is also discussed based on the results of the calculations of the Finite Difference Time Domain (FDTD) method.

CONTENTS

LIST OF FIGURES

Chapter 1

MOTIVATION

For centuries we have known the tried and tested idea of being able to obtain substances with desired features by altering their mechanical and electrical properties. Examples would involve the wide production and use of alloys, ceramics or the transistor revolution in electronics and the use of high temperature superconductors. But, today, the semiconductor electronics industry face the emerging challenge of improving the integrated device performance while struggling to minimize the size of the device.[1] Significant improvement can be achieved in this regard if one turns to other media, for example, the optical media.[2,3] Studies show a growing demand for an increase in the capacity of communication, for which many fields are being taken into consideration, one of which includes the optical medium.

Over the last few decades, a new door has opened in the optical media. Where, by controlling the optical properties of a material, and by clever use of the principles of reflection, refraction and superposition of light, scientists have been able to start a new revolution in our world of technology- known as Photonic Crystals, which are periodic dielectric structures. They are called crystals because of the periodicity and photonic because they act on light. Photonic crystals are also found in nature. For instance, the pattern on the butterfly's wing and its rainbow play is caused by the light reflection from the microstructure on the wing. Photonic crystals, in which the propagation of electromagnetic waves is forbidden for a specific frequency range, provide a promising tool to control the flow of light in integrated optical devices. [4,5] Growing interests have been shown in the last few years in the design and optimisation of photonic crystal based components such as waveguides,[6] lasers[7], splitters, fibres, [8] etc. One such photonic crystal based optical device is the waveguide based optical filter.

Optical devices are already in wide use, with optical fibre being a main player due to the speed of data transfer and data rates it can handle. But, with glass optical fibre, there always remains the need for electronic circuits in order to encode and decode the light signals for processing. For instance, if light signals of multiple wavelengths propagating through a glass optical fibre are in need of separation, they need to have to go through electronic processing for the demultiplexing, thereby introducing unwanted delay and complication in design. However, with photonic crystal filters or demultiplexers, the need for the electronic processing is reduced to zero, and light signals can be demultiplexed or filtered as desired through the photonic crystal filters in their optical state. These photonic crystal filters, working along with photonic crystal optical fibres has a scope of achieving much higher capacity by means of wavelength division multiplexing in the fields of communication.

Photonic crystal optical filters have been a topic of extensive research for quite some time now. Several methods of light filtering through photonic crystal have been proposed by researchers, including the cavity approach, resonance theory approach, self imaging, etc. This thesis deals with the photonic crystal waveguide approach to the study of optical filters.

In this thesis, we have proposed a design of a frequency splitting device, or optical filter with a two dimensional (2D) Photonic Crystal for light waves, by means of using waveguides. The work in thesis paper is heavily reliant on the concept of photonic band gaps (PBG).

This thesis is comprised of 4 more chapters that follow, where in chapter 2 an overview of what photonic crystal is about and discussion about its basic physical properties, including the 2D structure is given. This has been done so that one can get a fundamental idea about photonic crystals which would help to better understand further chapters in the thesis.

Chapter 3 intends to build a concept about the different computational methods which are widely used for photonic crystals as well as the modelling tools which are to be used in analysis and design of photonic crystals.

Chapter 4 is the core of this thesis, comprising of a detailed explanation on the work in this thesis paper. It talks about the idea behind the chosen design, corroborated by results of the computation methods discussed in chapter 3. Finally, a section in this chapter is dedicated to the optimisation of our device and evidences showing a better output.

Chapter 5 is the concluding chapter, where a discussion about the results of the work and scopes of future research on this topic is present.

Chapter 2

A BRIEF INTRODUCTION TO

PHOTONIC CRYSTALS:

BASIC CONCEPTS

2.1: Photonic crystals and its basic properties

A crystal is a periodic arrangement of particles- atoms, molecules or ions. The patterns with which these particles are repeated form the crystal lattice. An electron passing through a crystal lattice experiences a periodic potential. Both the elements of the crystal and the arrangement of the lattice indicate the conduction properties of the crystal.

Electrons propagate as waves and the energy of an electron in an atom is quantized and can have only certain discrete values. The same concept can be applied to the electron energy in a molecule or a crystal with several atoms. When atoms are brought close together to form a crystal, their inter-atomic interactions result in the formation of electron energy bands, mainly two distinct bands (Kasap, et.al 2001) It is because of this bandgap, that waves that fulfil certain criteria are able to travel through a periodic potential without scattering and also propagate through it while others are restricted.There are no allowed electron energies in the bandgap- it represents the forbidden electron energies in the crystal. The gap can extend to cover all possible directions of propagation of an electron if the lattice potential of the crystal is strong. Hence, this would result in a complete bandgap. A good example of such a material would be a semiconductor.

In a semiconductor, the electron energy in the crystal falls into two distinct energy bands called the valence band and the conduction band that are separated by the energy bandgap or the forbidden energy, as shown in the figure 2.1.

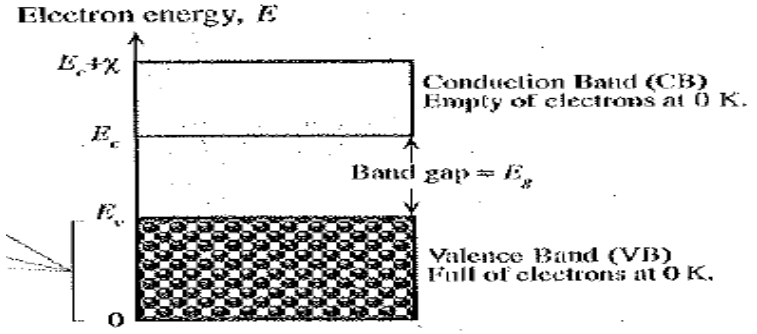

Fig2.1: The energy band diagram of electrons in a semiconductor (Source: Kasap, et.al 2001)

So, in order to make the understanding of the properties of photonic crystals less complicated, its optical analogy to crystals is considered.

In case of photonic crystals, the particles- atoms, molecules or ions are replaced by materials having different dielectric constants and the periodic dielectric function would replace the periodic potential of a crystal (Joannopoulos, et.al 1998). It is found that if the material being used has high efficiency (lossless medium), and if the dielectric constants of the different medium being used, varies considerably from each other, then the reflections and refractions of light by the interfaces of the photonic crystal allow photons to produce different phenomenon, similar to the ones that can obtained due to the periodic potential experienced by

electrons within a crystal. The most important property which determines significance of the photonic crystal is the photonic band gap.

The photonic band gap (PBG) corresponds to the energy or frequency range of light whose propagation is prohibited inside the photonic crystal, similar to the bandgap found in semiconductors. From the knowledge of semiconductors it can be understood that, when photons with energy, inside the PBG are incident on the structure, it is reflected back. However, if defects are introduced into the periodic structure, the effect would be same as the effect of introducing the defect to the crystal structure of a semiconductor. Thus, the radiation within the defect frequency will propagate inside the structure and in case of multiple defects, radiation will be guided like a waveguide (Joannopoulos, et.al 1998) Hence, it can be said that the photonic crystal is a low loss periodic dielectric material with presence of photonic bandgap which allows light of certain frequencies to travel and prevents propagation of others.

Based on the arrangement of the elements in the lattice, photonic crystals can be divided into three categories, namely one dimensional (1D), two dimensional (2D) and three dimensional (3D).

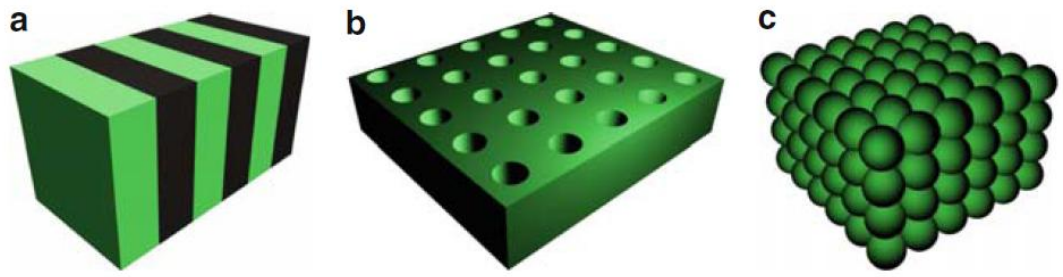

Fig2.2: Examples of a) 1D b) 2D c) 3D photonic crystal (Source: Sukhoivanov, et.al 2009)

In 1D photonic crystal, the periodicity exists in one direction only, whereas in the other two directions it is uniform. The 1D photonic crystal is comprised of alternating layers of materials with different dielectric constants. Example of this can be given as the Bragg mirror, or the multilayer dielectric mirror such as the quarter wave stack. In these devices, light wave at each interface is partially reflected and if the reflections from multiple interfaces interfere destructively, it would eliminate the forward propagating wave. On the other hand, if the interference is constructive, then a large percentage of the incident light will undergo reflection (Kasap, et.al 2001). The 1D photonic crystal is also used as anti reflecting coatings in order to improve the quality of optical devices. A 1D photonic crystal can have very few variations in its photonic structure, since it has a layered structure, hence only the number of layers, refractive index of each layer and the thickness of layers could be varied to bring about changes.

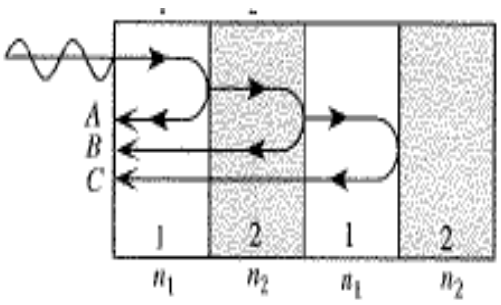

Fig2.3: The principle of dielectric mirror (Source: Kasap, et.al 2001)

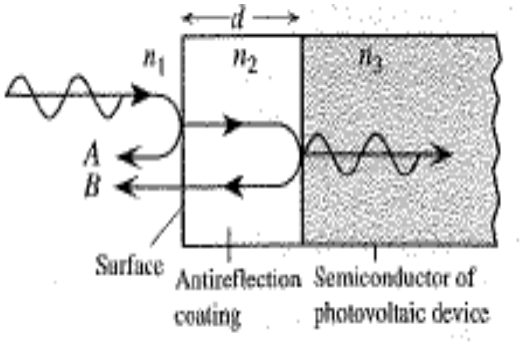

Fig2.4: Illustration of how an anti reflecting coating works (Source: Kasap, et.al 2001)

A 2D photonic crystal shows periodicity in two directions while uniform in the third direction. Photonic band gap appears in the planes of periodicity. A further detail about the 2D photonic crystal will be discussed later in this chapter.

Periodicity existing in all three planes forms the 3D photonic crystals. The number of possible ways to bring about changes in a 3D photonic crystal is much more when compared to 1D or 2D photonic crystal. By changing the arrangement of elements of 3D photonic crystals, one can create new form of applications. The example of naturally occurring 3D photonic crystal is the stone opal, which is famous for its unique optical properties such as showing off different colours when turned around. This is due to its reflectance property which depends on the incident angle of light, which is then reflected at different wavelengths creating the phenomenon. The geometry of 3D photonic crystals can be varied in different ways so that they can have various lattice structures. The similarity between the physics of photonic crystal and solid-state physics gives the possibility to provide the analogy between some properties and computation methods applied to solid-state and photonic crystal physics.

2.2: Reciprocal lattice and First Brillouin zone

In order to understand the operation of optical devices, it is very important to know how the electromagnetic field would interact with the photonic crystal device. For this reason, it is necessary to consider the distribution of electromagnetic field inside the lattice. Hence, to have an idea about photonic crystals and also in order to design photonic crystal based devices the use of reflectance spectrum, transmittance spectrum or the band structure of the crystal can be considered. It is best suited if band structures are used, since they provide complete information about electromagnetic waves propagating in the crystal.

The first step in this process would be to find out the parameters which would describe the structure of a photonic crystal. This includes terms such as unit cell, lattice vector, reciprocal lattice, reciprocal lattice vectors and the first Brillouin zone. The above terms will be explained in this chapter using the 1D or 2D structures for simplicity.

Unit Cell:

Photonic crystal is comprised of an infinite periodic structure. So it follows that, if the information of a single unit cell is understood than the information can be replicated to understand the entire structure. In other words, a unit cell is any region in space which, when translated, maps out the entire function of the crystal. In the region for a unit cell, a base point is selected and each point within the unit cell is closer to this base point rather than the neighbouring base points. The photonic crystal lattice is determined by its unit cell, its shape and permittivity (Sukhoivanov, et.al 2009).

The following method is used to determine a unit cell of a photonic crystal (Sukhoivanov, et.al 2009)

1. At first the base element of the photonic crystal has been selected. If the photonic crystal is comprised of rods in air then a single rod can be chosen as the base element.

2. Line segments are drawn to connect the base point with corresponding points of neighbouring elements.

3. Straight lines are drawn through the centre of each of the previously drawn line segments and perpendicular to them.

4. The figure formed by these lines form the unit cell of the photonic crystal.

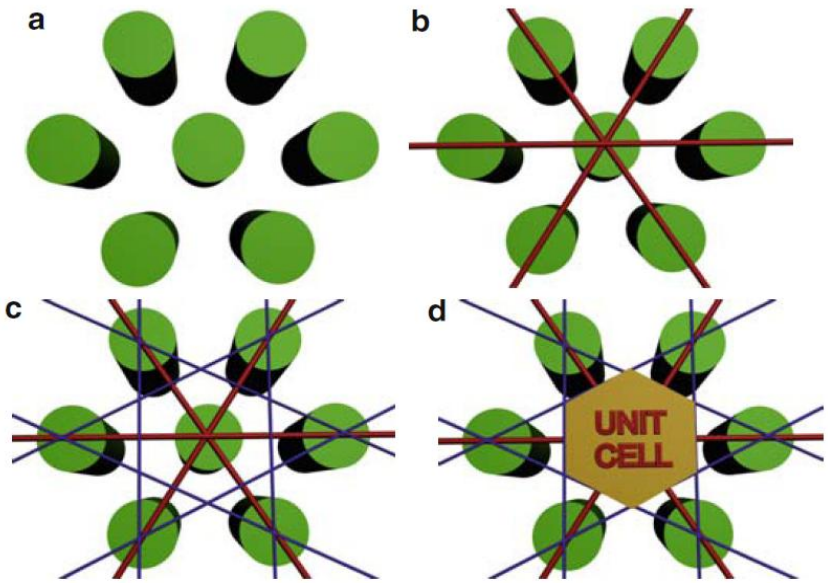

Fig2.5: Process of unit cell determination (Source: Sukhoivanov, et.al 2009)

Lattice Vector:

As mentioned before, the unit cell is translated to map out the entire function of the photonic crystal. The translation depends on the lattice vector. A lattice is a set of discrete points in space that repeats periodically. It should be chosen in such a way that it fills the entire unit cell. Since the photonic crystal has an infinite periodic structure, it is not possible to define an infinite number of lattice vectors. So a set of basis vectors, i.e. primitive lattice vector is defined. Its number is same as the number of dimension of the crystal (Sukhoivanov, et.al 2009). The lattice vector can be written in the general form
R = l**a1** + m**a2** + n**a3**, for some integers l, m and n. The point **R** is known as lattice vector, while the basis vector, a1, a2 and a3 are termed primitive lattice vectors.

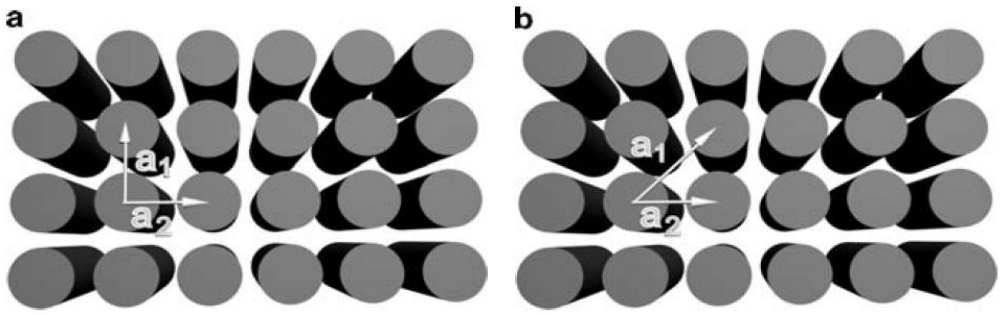

Fig2.6: Possible choices of primitive lattice vectors (Source: Sukhoivanov, et.al 2009)

Reciprocal lattice:

With every lattice there is a second lattice associated, termed the reciprocal lattice. The lattice and reciprocal lattice are the inverse of each other. The lattice vectors have the dimensions of length and so, the reciprocal lattice vectors have dimensions of inverse length. The lattice and reciprocal lattice are related by the equation:

$$ai \cdot bi = \delta ij 2\pi,$$

the derivation to which will be explained in the next chapter.

The reciprocal lattice vector is defined in terms of the basis primitive lattice vectors as done previously for establishing lattice vectors. From the primitive lattice vectors of the photonic crystal, the primitive reciprocal lattice vectors can be obtained.

The Brillouin Zone:

The unit cell of the reciprocal lattice is known as the first Brillouin Zone or simply the Brillouin Zone. It is determined in a similar manner as it has been done previously for the unit cell of the lattice vector in space. The process involved in establishing the Brillouin zone involves several steps (Sukhoivanov, et.al 2009):

1. Unit cell of the photonic crystal is determined.

2. Primitive lattice vector is set.

3. Primitive reciprocal lattice vectors are computed.

4. The base element of the photonic crystal, reciprocal lattice, is selected.

5. Line segments are joined to the point of the base element with corresponding points of neighbour elements.

6. Straight lines are drawn through the centre of each of the previously drawn line segments and perpendicular to them.

7. The region that developed is the Brillouin Zone.

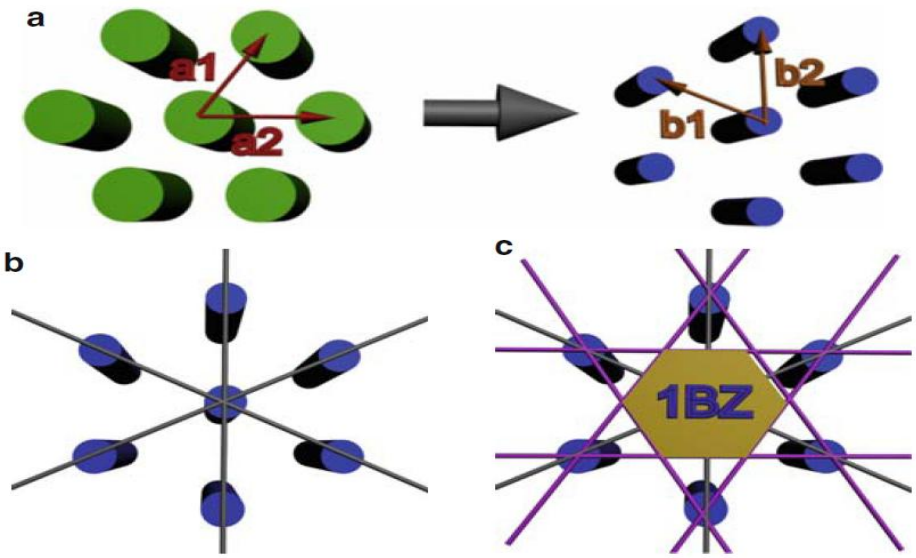

Fig2.7: The Brillouin Zone for a 2D photonic crystal (Source: Sukhoivanov, et.al 2009)

The reciprocal lattice and the Brillouin zone play a major role in the computation process of the photonic crystal band structure. It allows obtaining the limits of the variation of the wave vectors where computation of the eigen-states will be carried out. Within a Brillouin zone, there exist points, known as the high symmetry points, which could be translated into themselves only when rotating the Brillouin zone by 90°, 180°, 30° *or* 60° depending on the photonic crystal lattice. Computation of the band structure starts from the centre of the Brillouin zone and is denoted by" Γ" At this point the wave vector, k is zero. The computation then follows through all the high symmetry points and then returns to this point. This forms the k-path.

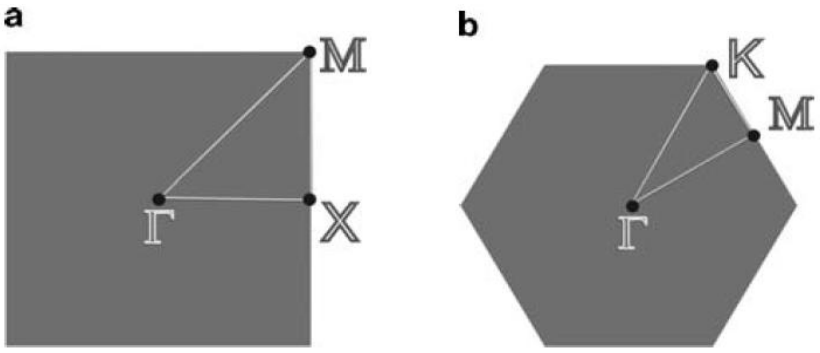

Fig2.8: K-path of photonic crystal with square and hexagonal lattice
(Source: Sukhoivanov, et.al 2009)

The square and hexagonal lattice of a 2D crystal will be discussed in the next section.

2.3: Two Dimensional Photonic crystals:

A two dimensional photonic crystal is periodic along two of its axes and has uniform periodicity along the third, the band gap appears in the plane of periodicity. Details about the photonic band gap in 2D crystals will be discussed in the next section. If light propagates in this plane, then it is possible to divide the harmonic modes into two independent polarizations, each of them having their own band structure. It can also prevent the propagation of light in any direction within the plane, unlike the 1D crystal.

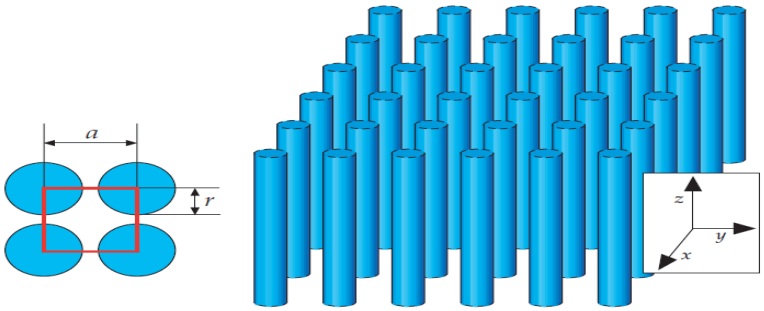

Fig2.9: A square lattice of dielectric column, with 'r' and 'a' shown on left
(Source: Joannopoulos, et. al 1998).

According to the figure 2.9, the columns are considered to be infinitely long. For certain values of the lattice constant, "a" (column spacing), the crystal can have a photonic band gap along the x and y axis. Within this gap, no states are permitted and the incident light is reflected.

Due to the variation of the shape of the elements and their placement, it is obvious that there are an infinite number of lattice types available for a 2D photonic crystal. However, in general, there are two commonly used lattice types of the 2D photonic crystal, the square and the hexagonal type. The unit cell of a square lattice 2D photonic crystal has the shape of a square and in case of hexagonal lattice, the unit cell has the shape of a regular hexagon.

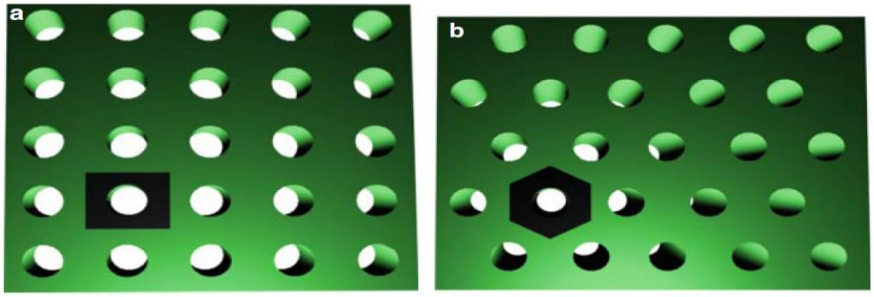

Fig2.10: Examples of 2D photonic crystal lattice types (Source: Sukhoivanov, et.al 2009)

2.4: Photonic band structure and band gap

As mentioned before, that the most important feature of the photonic crystal is its band gap. It corresponds to the range of light frequency or energy that is not allowed to propagate through the photonic crystal structure. However, if defects or irregularities are introduced it is possible to guide these forbidden energies by means of a waveguide.

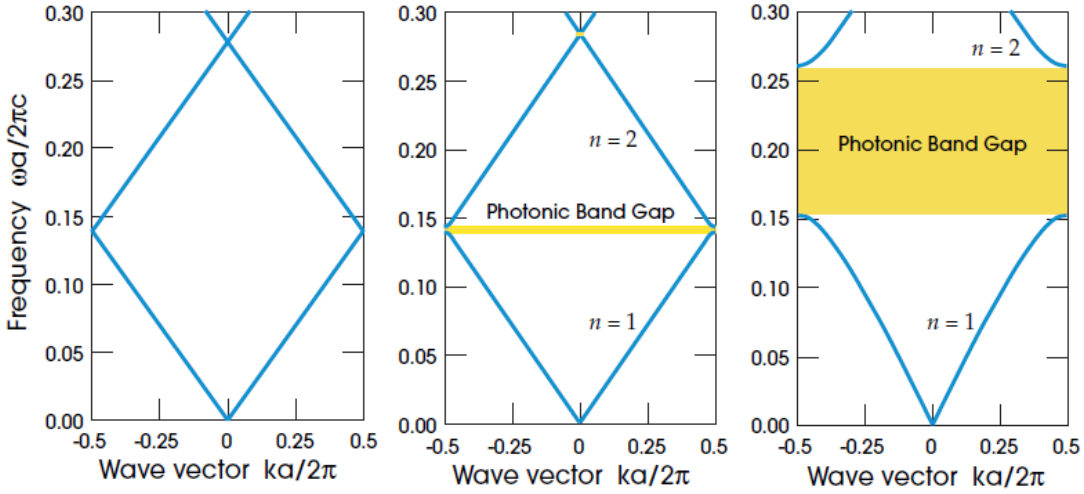

Fig2.11: The photonic band structure for on axis propagation as computed for 3 different multilayer films. (Source: Joannopoulos, et. al 1998).

The leftmost diagram in figure 2.11 is for a homogenous medium, i.e. all the layers have the same dielectric constant. The middle one is for a structure where alternate layers have dielectric constants of 13 and 12. The rightmost one is for a multilayer whose alternate layers have dielectric constants in the ratio 13:1. It is found that if other parameters are kept constant, then the band gap increases with increase in dielectric constant.

The problem associated with band structure computation of a photonic crystal is to find the dispersion relation, that is, the dependence of resonant frequencies of the photonic crystal on the wave vector of the radiation passing through it. In order to obtain the dispersion relation, it is necessary to solve the eigen problem equation inside infinite periodic structure, which will be discussed later in chapter 3.

The size of the band gap:

The scale of the crystal is an important factor while determining the extent of its band gap. For this reason, the extent of the band gap cannot be characterized by only considering its frequency width. Thus, the gap-mid gap ratio is used to determine the extent, since it is independent of the scale factor of a crystal. Let the frequency width of the band gap be $\Delta\omega$ and ω_m be the frequency at the middle of the gap, then gap-mid gap ratio is$\Delta\omega/\omega_m$. If the system undergoes scaling all the frequencies undergo scaling by the same factor and the gap- mid gap ratio remains the same. For this reason, in band diagrams the frequency and wave vector are plotted in dimensionless units $\omega a/2\pi c$ and $ka/2\pi c$, where frequency is equal to a/λ and λ is wavelength in vacuum.

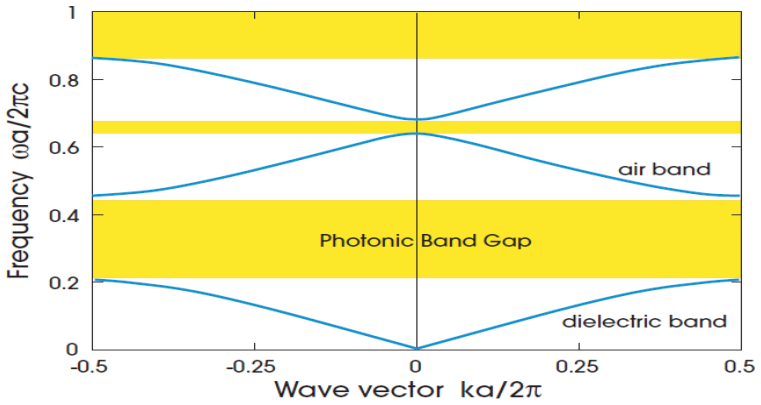

Fig2.12: The photonic band structure of a multilayer film (Source: Joannopoulos, et. al 1998).

Analysis of the band structure:

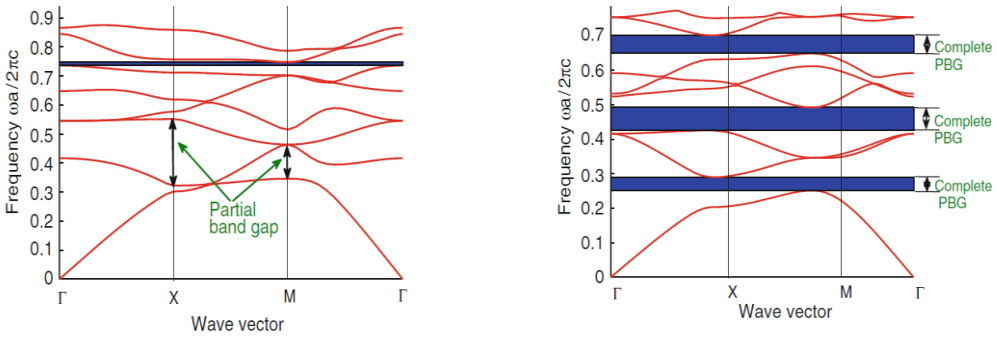

Fig2.13: Complete and partial photonic band gaps (Source: Sukhoivanov, et.al 2009)

As mentioned earlier, the wave vector space could be connected to the coordinate space by connecting some points of the Brillouin Zone with the radiation propagation direction within the photonic crystal. Hence it could be claimed that within each direction of the photonic crystal there exists a band gap, and these specific areas are referred to as the partial photonic band gaps. At some points these band gaps exist in all possible angles by overlapping with each other and hence creating the complete photonic band gap. Therefore, any one of the mentioned ways, by calculating the gap- mid gap ratio or by specifying the frequencies where photonic band gap appears, it is possible to locate the band gap in a photonic crystal.

Photonic Band Gap Maps:

During the designing process of a photonic crystal based device, it is important to determine photonic crystal parameters from known frequency characteristics. For example, in order to design the device with the band gap at the required frequency, it is important to be aware of the permittivity of the materials, the structure and size of elements being used or about the crystal lattice. To solve these problems, the photonic band gap map or the reduced band structure is used. The map is obtained by projecting the complete band gap, obtained at different values of the photonic crystal parameters such as refractive index, elements size, frequency etc.

The band gap map is drawn by gathering information about the complete band gap from the band structure and then plotting it against the ratio: radius/lattice constant.

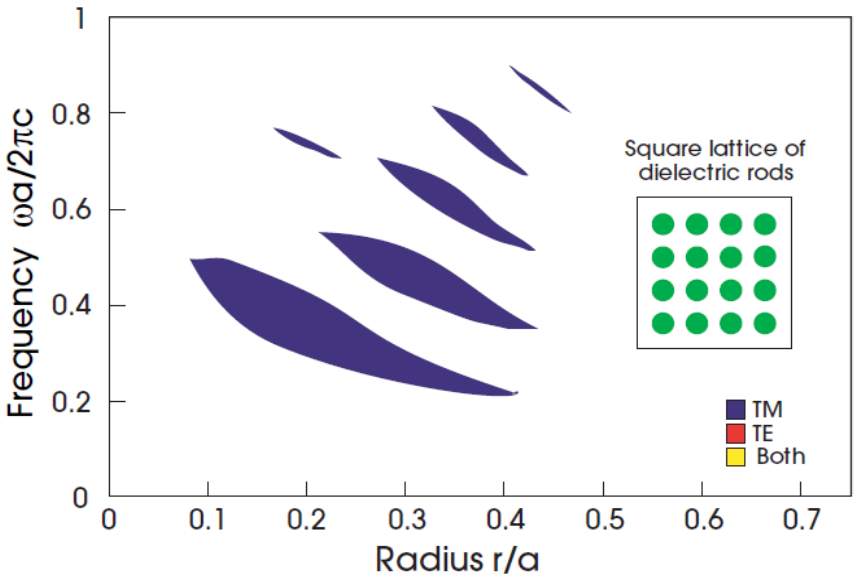

Fig2.14: Gap map for a square lattice of dielectric rods (Source: Joannopoulos, et. al 1998).

The photonic band gap map can be used to overcome a large number of problems during the designing process of the PhC devices. These maps could also be used to determine parameters at which maximum reflectance can be obtained. In chapter 4, much more of this band gap map is presented, as this is used as the main tool in the design of the device in this thesis.

Chapter 3

COMPUTATION METHODS USED:

PLANE WAVE EXPANSION (PWE)

&

FINITE DIFFERENCE TIME DOMAIN (FDTD)

3.1 Common terms used in computational methods

Before the Plane Wave Expansion method is discussed which is used for band gap calculation and the FDTD method which is used to find the field distribution inside the photonic crystal, some common terms are explained which are frequently used in these computational methods.

3.1.1 Eigen values and eigen vectors of a matrix

The general form of a matrix eigen problem is,

$$Ax = \gamma x \qquad (3.1.1.1)$$

where $A = \left|a_{i,j}\right|^n$ is a square matrix, γ are the eigen-values of the matrix and x are the eigen-vectors of the matrix corresponding to the specific eigen-values.

The eigen-vectors are represented as,

$$x = \sum_{i=1}^{n} x_i\, e_i \quad where \;\; e_i = e_1, e_2, \cdots, e_n \qquad (3.1.1.2)$$

Substituting equation (3.1.1.2) in equation (3.1.1.1) a system of scalar equations are obtained,

$$\left.\begin{matrix} a_{11}x_1 + a_{12}x_2 + \cdots + a_{1n}x_n = \gamma x_1 \\ \vdots \\ a_{n1}x_1 + a_{n2}x_2 + \cdots + a_{nn}x_n = \gamma x_n \end{matrix}\right\} \qquad (3.1.1.3)$$

Equations (3.1.1.3) can be written as,

$$\left.\begin{matrix} (a_{11} - \gamma)x_1 + a_{12}x_2 + \cdots + a_{1n}x_n = 0 \\ a_{21}x_1 + (a_{22} - \gamma)x_2 + \cdots + a_{2n}x_n = 0 \\ \vdots \\ a_{n1}x_1 + a_{n2}x_2 + \cdots + (a_{nn} - \gamma)x_n = 0 \end{matrix}\right\} \qquad (3.1.1.4)$$

The determinant of the system of equations (3.1.1.4) is set to zero,

$$\begin{bmatrix} a_{11} - \gamma & \cdots & a_{1n} \\ \vdots & \ddots & \vdots \\ a_{n1} & \cdots & a_{nn} - \gamma \end{bmatrix} = 0 \qquad (3.1.1.5)$$

The above determinant of equation 3.1.1.5 represents an algebraic equation of nth order which is called the characteristic equation. Each eigen-value is the root of the characteristic equation. When each eigen-value is substituted in equations (3.1.1.4) and solved, corresponding eigen-vector is obtained.

3.1.2 The Helmholtz equation

The Helmholtz equation is,

$$\nabla^2 A + k^2 A = 0 \ \ where\ \nabla^2\ is\ the\ Laplace\ operator, k\ is\ the\ wave\ number\ and\ A\ is\ the\ amplitude.$$

Helmholtz equation is used to solve partial differential equations in time and space. The Helmholtz equation emerges from applying the technique of separation of variables to make the solution easier.

Starting with the wave equation,

$$\left(\nabla^2 - \frac{1}{c^2}\frac{\partial^2}{\partial t^2}\right) u(r,t) = 0 \qquad (3.1.2.1)$$

The wave function $u(r,t)$ is then separated,

$$u(r,t) = A(r)T(t) \qquad (3.1.2.2)$$

Substituting equation (3.1.2.2) in equation (3.1.2.1) the following equation is obtained,

$$\frac{\nabla^2 A}{A} = \frac{1}{c^2 T}\frac{d^2 T}{dt^2} \qquad (3.1.2.3)$$

$-k^2$ is chosen to be equal to the left and right hand side of equation (3.1.2.3) where k is the wave number,

$$\frac{\nabla^2 A}{A} = -k^2 \qquad (3.1.2.4)$$

$$\frac{1}{c^2 T}\frac{d^2 T}{dt^2} = -k^2 \qquad (3.1.2.5)$$

Rearranging equation (3.1.2.4) we get,

$(\nabla^2 + k^2)A = 0$, which is a Helmholtz equation for spatial variable r.

Substituting $c = \frac{\omega}{k}$, where ω is the angular frequency, equation (3.1.2.5) becomes,

$\left(\frac{d^2}{dt^2} + \omega^2\right) T = 0$, which is a second order differential Helmholtz equation for time.

3.1.3 The Hermitian Matrix

A Hermitian matrix is a square matrix with complex entries that is equal to its own conjugate transpose. The element in the ith row and jth column is equal to the complex conjugate of the jth row and ith column. For a Hermitian matrix A, $A_{ij} = \overline{A_{ji}}$.

The following is an example of a Hermitian matrix, $\begin{bmatrix} 5 & 3+i & 6 \\ 3-i & 8 & i \\ 6 & -i & 7 \end{bmatrix}$.

3.2 The Plane Wave Expansion Method

The plane wave expansion method is a technique which uses an eigen formulation of the Maxwell's equations and solves the eigen frequencies for each of the propagation directions of the wave vectors in a photonic crystal. (Danner et.al 2011)

Plane Wave Expansion (PWE) method is used for calculating electromagnetic band gaps (Satpathy, et al. 1990). It can also be used to simulate the field distribution in photonic crystals but the FDTD method (explained in section 3.4) is preferred to calculate the field distribution because the FDTD algorithm does not need to solve integral equations and it is easier to obtain frequency domain data from time domain results rather than the converse. When many frequencies are involved the frequency domain can be more easily obtained from the time domain.

Evaluation of the Plane Wave Expansion Method starts with the **Maxwell**'s equations. The following derivations of equations are for 2D photonic crystals.

For the following equations the meaning of the symbols are as follows,

$\nabla.$: Divergence operator

$\nabla \times$: Curl operator

B: Magnetic flux density or magnetic field density or magnetic induction measured in tesla (T)

H: Magnetic field strength or magnetic field measured in ampere per meter (A/m)

D: Electric displacement field or electric flux density measured in coulomb per square meter (C/m^2)

E: Electric field measured in newton per coulomb (N/C)

J: Current density measured in ampere per meter square (A/m^2)

ρ: Electric charge density measured in coulomb per meter square (C/m^2)

$$\nabla . D = \rho \qquad (3.2.1)$$

$$\nabla . B = 0 \qquad (3.2.2)$$

$$\nabla \times E = -\frac{\partial B}{\partial t} \qquad (3.2.3)$$

$$\nabla \times H = J + \frac{\partial D}{\partial t} \qquad (3.2.4)$$

It is assumed there is no charge and current density in a 2D photonic crystal.

$$\nabla . E = 0 \tag{3.2.5}$$

$$\nabla . H = 0 \tag{3.2.6}$$

$$\nabla \times E = -\mu\mu_0 \frac{\partial H}{\partial t} \tag{3.2.7}$$

$$\nabla \times H = \varepsilon\varepsilon_0 \frac{\partial E}{\partial t} \tag{3.2.8}$$

Where, $D = \varepsilon\varepsilon_0 E$ and $B = \mu\mu_0 H$.

μ= Permeability in Am^2 and μ_0= Permeability of free space in Am^2

ε= Permittivity in F/m and ε_0= Permittivity of free space in F/m

With equations 3.2.7 and 3.2.8 it can be written that,

$$\nabla \times n\nabla \times H + \frac{\mu}{c^2}\frac{\partial^2 H}{\partial t^2} = 0 \tag{3.2.9}$$

Here $n = \frac{1}{\varepsilon}$ and $c = \frac{1}{\sqrt{\mu_0 \varepsilon_0}}$

H is written as inverse Fourier transform in time and space,

$$H(r,t) = \iint H\left(k^{'},\omega\right) e^{i\left(k^{'}.r-\omega t\right)} dk^{'} d\omega \tag{3.2.10}$$

$k^{'}$ is the wave vector in the material.

A plane wave of frequency ω is,

$$E(r,t) = E_0 e^{i(k.r-\omega t)} \tag{3.2.11}$$

Thus it can be inferred that equation 3.2.10 is summation of plane waves with infinite frequencies and wave vectors. This is the basic equation for plane wave expansion.

Equation 3.2.10 is used in equation 3.2.9 and the new equation formed is,

$$\nabla \times n\nabla \times H(r,\omega) - \frac{\omega^2 \mu}{c^2} H(r,\omega) = 0 \tag{3.2.12}$$

$$\text{Where, } H(r,\omega) = \int H\left(k^{'},\omega\right) e^{ik^{'}.r}\, dk^{'} \tag{3.2.13}$$

$k^{'}$ and r are in the y-z plane.

Next the equations defining the reciprocal lattice of a 2D photonic crystal are required to further develop the plane wave expansion method.

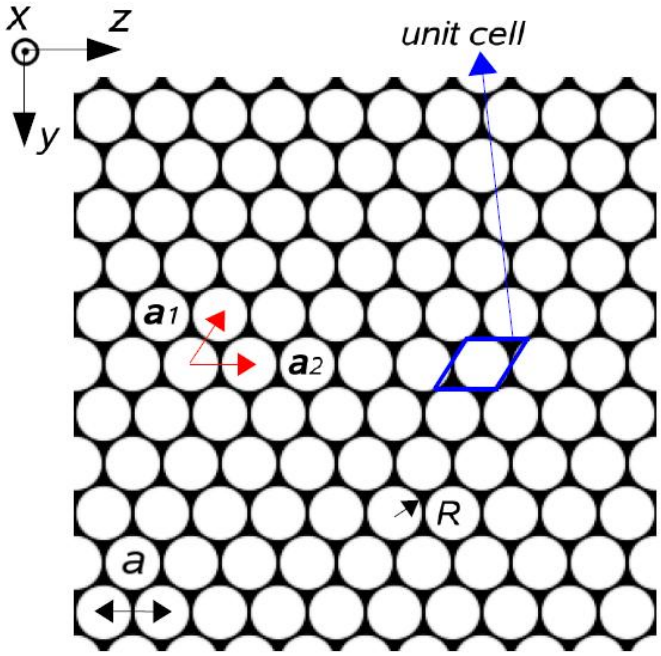

Fig3.1: Lattice of a 2D hexagonal Photonic crystal. R represents radius. (Source: Adam Enes Erol 2009)

The figure 3.1 shows the lattice of a 2D hexagonal photonic crystal where a_1 and a_2 are the basis vectors of the lattice. The blue enclosure defined by the basis vectors is the unit cell.

The translational vector in the lattice is,

$$R=n_1a_1+n_2a_2 \qquad (3.2.14)$$

$n_1, n_2 \in$ integers.

Because of the periodicity of the lattice,

$$(r) = n(r + R) \qquad (3.2.15)$$

$$\mu(r) = \mu(r + R) \qquad (3.2.16)$$

The reciprocal lattice vector called G is,

$$G=m_1b_1+m_2b_2 \qquad (3.2.17)$$

$m_1, m_2 \in$ integers.

b_1 and b_2 are the basis vectors of the **reciprocal lattice** (shown in the figure 3.2).

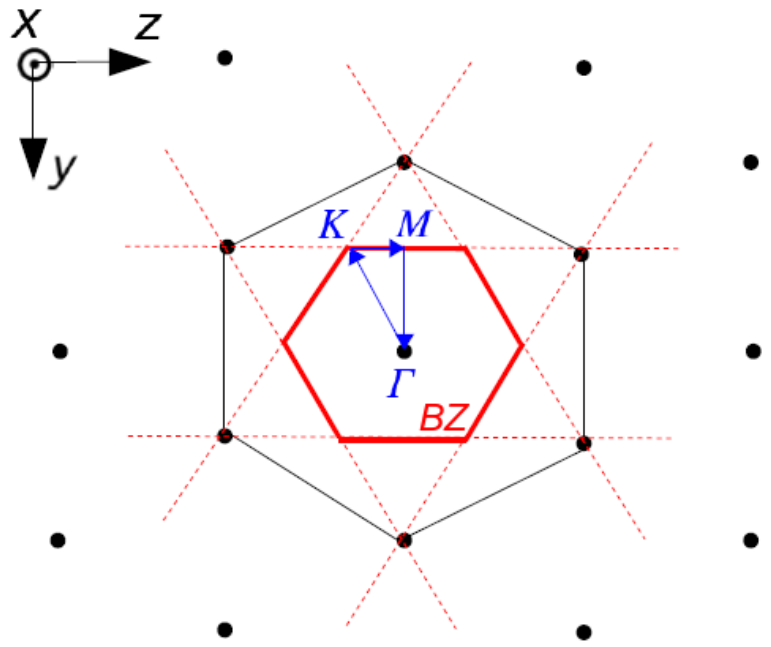

Fig3.2: Reciprocal lattice of a 2D hexagonal photonic crystal. BZ stands for Brillouin zone. (Source: Adam Enes Erol 2009)

$$b_1 = 2\pi \frac{a_2 \times \hat{x}}{a_1 . a_2 \times \hat{x}} \qquad (3.2.18)$$

$$b_2 = 2\pi \frac{\hat{x} \times a_1}{a_1 . a_2 \times \hat{x}} \qquad (3.2.19)$$

$$a_i . b_j = 2\pi \delta_{ij} \qquad (3.2.20)$$

$n(r) and\ \mu(r)$ can be now written as Fourier series in terms of G,

$$n(r) = \sum_{G'} n(G') e^{iG'.r} \qquad (3.2.21)$$

$$\mu(r) = \sum_{G''} \mu(G'') e^{iG''.r} \qquad (3.2.22)$$

$k' = k + G$ is substituted in equation 3.2.13,

$$H(r, \omega) = \sum_G \int_{BZ} H(K + G, \omega) e^{i(k+G).r}\ dk \qquad (3.2.23)$$

BZ stands for Brillouin zone (shown in the figure 3.2), i.e. the unit cell of the reciprocal lattice.

This is similar to **Bloch's theorem** which states that the energy eigen-function for a system where the wave function of a particle is placed in a periodic potential is written as the product of a plane wave envelope function and periodic function ($u_{nk\,(r)}$) that has the same periodicity as the potential. The equation takes the following form,

$$\varphi_{nk\,(r)} = e^{ik.r} u_{nk\,(r)} \qquad (3.2.24)$$

The energy eigen-values are $\epsilon_n(k) = \epsilon_n(k+G)$ which is periodic with periodicity G of the reciprocal lattice vector. The energies associated with the index n differ with wave number k and form an energy band defined by band index n. The eigen-values for n are periodic in k and all values of $\epsilon_n(k)$ occur for k values within the first Brillouin zone.

Equations 3.2.17 to 3.2.23 are used in equation 3.2.13 to get a generalized eigen-value equation in terms of magnetic field H,

$$\sum_G n(G^{'} - G)\big(k + G^{'}\big) \times [(k+G) \times H(k+G,\omega)] + \frac{\omega^2}{c^2}\mu\big(G^{'} - G\big)H(k+G,\omega) = 0$$

Similarly the generalized eigen-value equation for electric field E is,

$$\sum_G \frac{1}{\mu}(G^{'} - G)\big(k + G^{'}\big) \times [(k+G) \times E(k+G,\omega)] + \frac{\omega^2}{c^2}\varepsilon\big(G^{'} - G\big)E(k+G,\omega) = 0$$

Using PWE method for computations can prove to be disadvantageous because as it follows the Fourier method it suffers from Gibb's phenomenon (the unusual manner in which the Fourier series of a piecewise continuous differentiable periodic function behaves at a discontinuity) and converges slowly to the solution. Despite its drawbacks PWE is the most widely used method for calculating band gaps and dispersion relations due to its ease of implementation.

3.3 Band Gap Calculation using Plane Wave Expansion

In Section 2.4 the Band Gap of a Photonic crystal was discussed. The Band Gap of a photonic crystal explains the behavior of the incident light while propagating in a specific direction inside the photonic crystal. In this section it is explained how the Band Gap is calculated using the Plane Wave Expansion Method. For simplicity the process to calculate the Band Gap for a 1D photonic crystal is shown. 2D photonic crystal band gap calculation follows a similar process.

It is required to solve the eigen-problem for Helmholtz equation in order to calculate the band gap. The Helmholtz equation in terms of magnetic field is,

$$\frac{\partial}{\partial x}\frac{1}{\varepsilon(x)}\frac{\partial}{\partial x}H(x) + \frac{\omega^2}{c^2}H(x) = 0 \qquad (3.3.1)$$

The eigen-function of an infinite periodic structure such as a photonic crystal is also infinitely periodic. Thus, the Bloch theorem is used to represent the eigen-function of the photonic crystal.

$$H(x) = h_{k,n(x)}.e^{(j.k.x)} \qquad (3.3.2)$$

Here $h_{k,n(x)}$ is a periodic function and n is the state number.

Equation (3.3.2) is expanded to Fourier series by reciprocal lattice vectors,

$$H(x) = \sum_{G} h_{k,n}\,(G).\, e^{j.(k+G).x} \tag{3.3.3}$$

$h_{k,n}$(G) is a periodic function in terms of wave vectors also known as Fourier expansion coefficient.

The dielectric function is also periodic, thus for convenience its reverse is taken as a Fourier series function,

$$\frac{1}{\varepsilon(x)} = \sum_{G"\in G} \aleph(G")e^{(j.G".x)} \tag{3.3.4}$$

$\aleph(G")$ is the Fourier expansion coefficient of the inverted dielectric function.

The infinite functions are substituted in equation (3.3.1) to get,

$$\sum_{G"} \frac{\partial}{\partial x}\aleph(G")e^{(j.G".x)}\frac{\partial}{\partial x}\sum_{G'} h_{k,n}\,(G').\, e^{j.(k+G').x)} + \frac{\omega^2}{c^2}\sum_{G} h_{k,n}\,(G).\, e^{(j.(k+G).x)} = 0 \tag{3.3.5}$$

Taking $G = G' + G"$ equation (3.3.5) takes the form of,

$$\sum_{G}\sum_{G'} \frac{\partial}{\partial x}\aleph(G - G')e^{(j.(G-G').x)}.\, h_{k,n}(G').\frac{\partial}{\partial x} e^{(j.(k+G').x)} + \frac{\omega^2}{c^2}\sum_{G} h_{k,n}\,(G).\, e^{(j.(k+G).x)} = 0 \tag{3.3.6}$$

Taking derivatives and combining the exponents the equation is,

$$\sum_{G}\sum_{G'} \aleph(G - G').\, h_{k,n}(G').\, e^{(j.(k+G).x).(j.(k+G').j.(k+G))} + \frac{\omega^2}{c^2}\sum_{G} h_{k,n}\,(G).\, e^{(j.(k+G).x)} = 0 \tag{3.3.7}$$

Due to the projection to the basis $e^{(j.(k+G).x)}$ equation (3.3.7) becomes,

$$\sum_{G'} \aleph(G - G')\big((k + G').\,(k + G)\big).\, h_{k,n}(G') + \frac{\omega^2}{c^2} h_{k,n}(G) = 0 \tag{3.3.8}$$

Equation (3.3.8) is not dependent on co-ordinates but only on the reciprocal lattice vector.

The operator in equation (3.3.8) can be represented in the form of a matrix, whose element can be found from the following equation,

$$\hat{\theta}_{G,G'} = \aleph(G - G')\big((k + G').\,(k + G)\big) \tag{3.3.9}$$

Set of solutions of system of equations (3.3.8) can be found as eigen-values of matrix differential operator,

$$\hat{\theta} = \begin{vmatrix} \hat{\theta}_{G_1 G_1'} & \cdots & \hat{\theta}_{G_N G_1'} \\ \vdots & \ddots & \vdots \\ \hat{\theta}_{G_1 G_N'} & \cdots & \hat{\theta}_{G_N G_N'} \end{vmatrix} \tag{3.3.10}$$

The set of G and G' should be the same so that the matrix is a square one.

Equation (3.3.10) is a Hermitian matrix. A Hermitian matrix has the following condition,

$$\hat{\theta}_{G,G'} = \hat{\theta}^*_{G',G} \qquad (3.3.11)$$

Equation (3.3.11) means that the diagonal-symmetric elements are complex conjugated. The eigen-value of the matrix is $\frac{\omega^2}{c^2}$ which gives the eigen frequency of the structure. The result of the eigen-problem solution is represented as a band structure as shown in Figure 3.3,

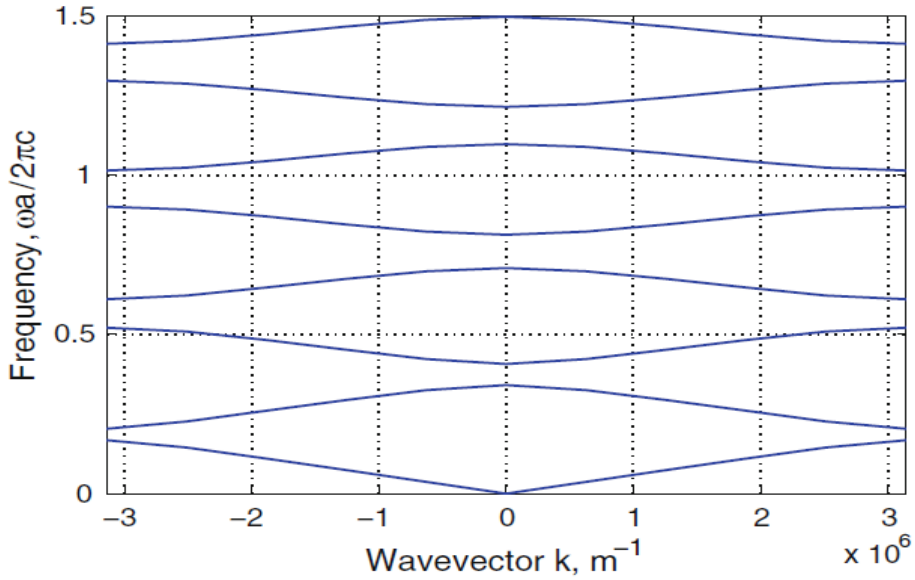

Fig3.3: Band structure of a 1D Photonic Crystal (Source: Sukhoivanov, et al. 2009)

The x-axis of the band structure represents the wave-vector and the y-axis represents the normalized frequency which is $\frac{\omega a}{2\pi c}$. The frequency is normalized by the period of the photonic crystal, so the scale of the structure does not matter. The period of the photonic crystal can be of micrometers of millimeters but the band structure remains unchanged regardless of the size of the period due to the normalized frequency. The layer thickness ratio and permittivity is kept constant in this case.

Analyzing the band structure of figure 3.3 in detail, the eigen-frequencies of the photonic crystal start from zero frequency at k=0. Higher on the frequency axis exists the photonic band gap. The photonic crystal does not have eigen-states within the photonic band gap. The bands and photonic band gaps appear consecutively on the frequency axis except when the photonic band gap width is almost equal to zero. In figure 3.3, for a 1D photonic crystal the appearance of the band gaps are very frequent but for a 2D photonic crystal band gaps appear much rarely.

3.4 Finite-Difference Time-Domain Method (FDTD)

Plane Wave expansion is used for eigen-states calculations for an infinite periodic structure in addition to calculations of field distributions which correspond to those states but it is not suitable when the need is to find field distribution in complicated structures or examine dynamic characteristics.

The FDTD method is one of the most advanced numerical analysis technique today for computation of the field distribution inside Photonic crystal devices. In this thesis the software RSoft Photonic CAD Suite uses FDTD to simulate the propagation of light in the photonic crystal.

FDTD method consists of discretization of space. The derivatives in Maxwell's equations are replaced by finite differences that results in a system of algebraic equations which are linear on coordinates. The system is solved sequentially starting from initial and boundary conditions. (Sukhoivanov, et al. 2009).

The FDTD method allows finding the field distribution by solving the system of Maxwell's equations on the discrete cell. The solution is based on the permittivity distribution function which determines radiation propagation conditions, initial conditions which contains radiation parameters such as the wavelength or the radiation spectrum for non-monochromatic wave, the amplitude and the initial phase, and boundary conditions which determine the radiation behavior at the boundary of the computation region (Sukhoivanov, et al. 2009). When these conditions are set, the field distribution is computed one by one.

The symbols in the equations that follow have the following meaning:

B: Magnetic flux density or magnetic field density or magnetic induction measured in tesla (T)

D: Electric displacement field or electric flux density measured in coulomb per square meter (C/m^2)

E: Electric field measured in newton per coulomb (N/C)

H: Magnetic field strength or magnetic field measured in ampere per meter (A/m)

c: Speed of light in vacuum measured in meters per second (m/s)

μ: Permeability measured in ampere square meter (Am^2)

ε: Permittivity measured in farad per meter (F/m)

Maxwell's Equations are taken to derive in terms of finite differences. The equations for the medium are considered neglecting dispersion, absorption or light generation:

$$\nabla \times E(r,t) = -\frac{1}{c}\frac{\partial B(r,t)}{\partial t}$$

$$\nabla \times H(r,t) = \frac{1}{c}\frac{\partial D(r,t)}{\partial t}$$

The curl operators are evaluated and the equations are written separately by their vector components. All the equations are in a single direction:

$$\frac{\partial E_z}{\partial y} - \frac{\partial E_y}{\partial z} = -\frac{1}{c}\frac{\partial B_x}{\partial t}$$

$$\frac{\partial E_x}{\partial z} - \frac{\partial E_z}{\partial x} = -\frac{1}{c}\frac{\partial B_y}{\partial t}$$

$$\frac{\partial E_y}{\partial x} - \frac{\partial E_x}{\partial y} = -\frac{1}{c}\frac{\partial B_z}{\partial t}$$

$$\frac{\partial H_z}{\partial y} - \frac{\partial H_y}{\partial z} = \frac{1}{c}\frac{\partial D_x}{\partial t}$$

$$\frac{\partial H_x}{\partial y} - \frac{\partial H_z}{\partial z} = \frac{1}{c}\frac{\partial D_y}{\partial t}$$

$$\frac{\partial H_y}{\partial y} - \frac{\partial H_x}{\partial z} = \frac{1}{c}\frac{\partial D_z}{\partial t}$$

FDTD is mainly based on discretization of space, thus all the partial derivatives are interchanged with differences:

$$\frac{\partial}{\partial x} \approx \frac{\Delta}{\Delta x}$$

$$\frac{\partial}{\partial y} \approx \frac{\Delta}{\Delta y}$$

$$\frac{\partial}{\partial z} \approx \frac{\Delta}{\Delta z}$$

The derivative is represented by its approximate value which is the function variation divided by the argument variation taken at different cell nodes as shown in figure 3.4.

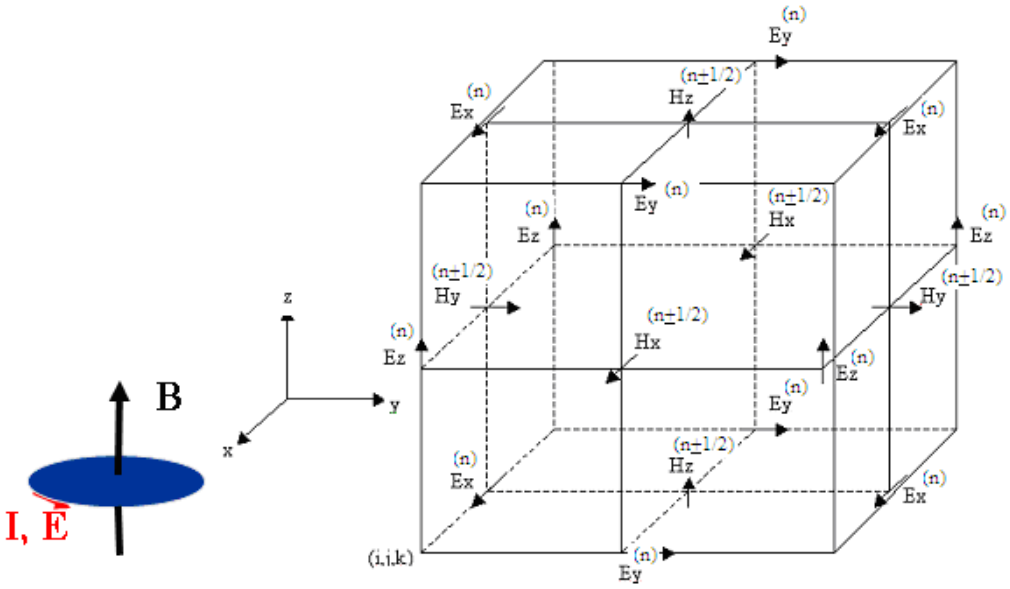

Fig3.4: Yee Cell used for FDTD method computation (Source: Farid, et.al 2011)

In the figure 3.4, a single cell is shown with all corresponding components of the field vectors. By solving the system of Maxwell's equations by the FDTD method, values of the field intensity in each cell node is obtained.

Replacing the derivatives by differences the recurrent expression is obtained which gives the value of the field component in a node of the cell using known values of the field components in adjacent nodes. The recurrent equations are:

$$H_{x(i,j,k)}^{n+1/2} = H_{x(i,j,k)}^{n-1/2} + \frac{c\Delta t}{\mu\Delta z}\left(E_{y\left(i,j,k+\frac{1}{2}\right)}^{n} - E_{y\left(i,j,k-\frac{1}{2}\right)}^{n}\right) - \frac{c\Delta t}{\mu\Delta y}\left(E_{z\left(i,j+\frac{1}{2},k\right)}^{n} - E_{z\left(i,j-\frac{1}{2},k\right)}^{n}\right)$$

$$H_{y(i,j,k)}^{n+1/2} = H_{y(i,j,k)}^{n-1/2} + \frac{c\Delta t}{\mu\Delta x}\left(E_{z(i+1/2,j,k)}^{n} - E_{z(i-1/2,j,k)}^{n}\right) - \frac{c\Delta t}{\mu\Delta z}\left(E_{x(i,j,k+1/2)}^{n} - E_{x(i,j,k-1/2)}^{n}\right)$$

$$H_{z(i,j,k)}^{n+1/2} = H_{z(i,j,k)}^{n-1/2} + \frac{c\Delta t}{\mu\Delta y}\left(E_{x(i,j+1/2,k)}^{n} - E_{x(i,j-1/2,k)}^{n}\right) - \frac{c\Delta t}{\mu\Delta x}\left(E_{y(i+1/2,j,k)}^{n} - E_{y(i-1/2,j,k)}^{n}\right)$$

$$E_{x(i,j,k)}^{n+1} = E_{x(i,j,k)}^{n} + \frac{c\Delta t}{\varepsilon\Delta y}\left(H_{z\left(i,j+\frac{1}{2},k\right)}^{n+\frac{1}{2}} - H_{z\left(i,j-\frac{1}{2},k\right)}^{n+\frac{1}{2}}\right) - \frac{c\Delta t}{\varepsilon\Delta z}\left(H_{y\left(i,j,k+\frac{1}{2}\right)}^{n+\frac{1}{2}} - H_{y\left(i,j,k-\frac{1}{2}\right)}^{n+\frac{1}{2}}\right)$$

$$E_{y(i,j,k)}^{n+1} = E_{y(i,j,k)}^{n} + \frac{c\Delta t}{\varepsilon\Delta z}\left(H_{z\left(i,j,k+\frac{1}{2}\right)}^{n+\frac{1}{2}} - H_{z\left(i,j,k-\frac{1}{2}\right)}^{n+\frac{1}{2}}\right) - \frac{c\Delta t}{\varepsilon\Delta x}\left(H_{y\left(i+\frac{1}{2},j,k\right)}^{n+\frac{1}{2}} - H_{y\left(i-\frac{1}{2},j,k\right)}^{n+\frac{1}{2}}\right)$$

$$E_{z(i,j,k)}^{n+1} = E_{z(i,j,k)}^{n} + \frac{c\Delta t}{\varepsilon\Delta x}\left(H_{z\left(i+\frac{1}{2},j,k\right)}^{n+\frac{1}{2}} - H_{z\left(i-\frac{1}{2},j,k\right)}^{n+\frac{1}{2}}\right) - \frac{c\Delta t}{\varepsilon\Delta y}\left(H_{y\left(i,j+\frac{1}{2},k\right)}^{n+\frac{1}{2}} - H_{y\left(i,j-\frac{1}{2},k\right)}^{n+\frac{1}{2}}\right)$$

The above equations show the step-by-step recurrent computation of the electric field and the magnetic field starting from one side of the computation cell and moving to the other side. The values of the electric and magnetic field components are taken at the nodes (i+1/2,

j+1/2, k+1/2) and (i–1/2, j–1/2, k–1/2) in order to take central differences approximation. Computation is carried out over and over again for different times till required computation time is achieved.

For a 2D photonic crystal either TM or TE polarization is considered.

In case of TM polarization there is a non-zero electric field component which is parallel to the photonic crystal and magnetic field components lying in the plane of the photonic crystal. All other electric and magnetic field components equal to zero.

$$\frac{\partial}{\partial y}E_z = -\frac{1}{c}\frac{\partial}{\partial t}B_x$$

$$-\frac{\partial}{\partial x}E_z = -\frac{1}{c}\frac{\partial}{\partial t}B_y$$

$$\frac{\partial}{\partial x}H_y - \frac{\partial}{\partial y}H_x = \frac{1}{c}\frac{\partial}{\partial t}D_z$$

Recurrent formula for computation of the field distribution taken in this case is of the following form,

$$H_{x(i,j)}^{n+1/2} = H_{x(i,j)}^{n-1/2} - \frac{c\Delta t}{\mu\Delta y}(E_{z\left(i,j+\frac{1}{2}\right)}^{n} - E_{z\left(i,j-\frac{1}{2}\right)}^{n})$$

$$H_{y(i,j)}^{n+1/2} = H_{y(i,j)}^{n-1/2} + \frac{c\Delta t}{\mu\Delta x}(E_{z\left(i,j+\frac{1}{2}\right)}^{n} - E_{z\left(i,j-\frac{1}{2}\right)}^{n})$$

$$E_{z(i,j)}^{n+1} = E_{z(i,j)}^{n} + \frac{c\Delta t}{\varepsilon\Delta x}\left(H_{y\left(i+\frac{1}{2},j\right)}^{n+\frac{1}{2}} - H_{y\left(i-\frac{1}{2},j\right)}^{n+\frac{1}{2}}\right) - \frac{c\Delta t}{\varepsilon\Delta y}(H_{x\left(i,j+\frac{1}{2}\right)}^{n+\frac{1}{2}} - H_{x\left(i,j-\frac{1}{2}\right)}^{n+\frac{1}{2}})$$

In case of TE polarization, magnetic field component which is parallel to the photonic crystal and electric field components lying in the plane of photonic crystal are non-zero. All other components equal to zero,

$$\frac{\partial}{\partial x}E_y - \frac{\partial}{\partial y}E_x = -\frac{1}{c}\frac{\partial}{\partial t}B_z$$

$$\frac{\partial}{\partial y}H_z = \frac{1}{c}\frac{\partial}{\partial t}D_x$$

$$-\frac{\partial}{\partial x}H_z = \frac{1}{c}\frac{\partial}{\partial t}D_y$$

Replacing the derivatives by differences the recurrent formulas below are obtained,

$$H_{z(i,j)}^{n+1/2} = H_{z(i,j)}^{n-1/2} + \frac{c\Delta t}{\mu\Delta y}\left(E_{x\left(i,j+\frac{1}{2}\right)}^{n} - E_{x\left(i,j-\frac{1}{2}\right)}^{n}\right) - \frac{c\Delta t}{\mu\Delta x}(E_{y\left(i+\frac{1}{2},j\right)}^{n} - E_{y\left(i-\frac{1}{2},j\right)}^{n})$$

$$E_{x(i,j)}^{n+1} = E_{x(i,j)}^{n} + \frac{c\Delta t}{\varepsilon\Delta y}(H_{z\left(i,j+\frac{1}{2}\right)}^{n+\frac{1}{2}} - H_{z\left(i,j-\frac{1}{2}\right)}^{n+\frac{1}{2}})$$

$$E_{y(i,j)}^{n+1} = E_{y(i,j)}^{n} + \frac{c\Delta t}{\varepsilon \Delta x}\left(H_{z(i+1/2,j)}^{n+\frac{1}{2}} - H_{z(i-1/2,j)}^{n+\frac{1}{2}}\right)$$

FDTD does not have any approximations or theoretical restrictions as it is a rigorous solution to Maxwell's equations. With FDTD when a broadband pulse such as a Gaussian pulse is used as the source, then the response of the system over a wide range of frequencies can be obtained with a single simulation.

FDTD calculates the E and H fields everywhere in the computational domain and as they develop with time, FDTD helps to provide animated displays of the electromagnetic field movement through the model. This display is useful in understanding what is happening in the model and ensures that the model is working correctly.

The FDTD algorithm follows the loop shown in figure 3.5 for as many values of n as we want till we reach our desired values.

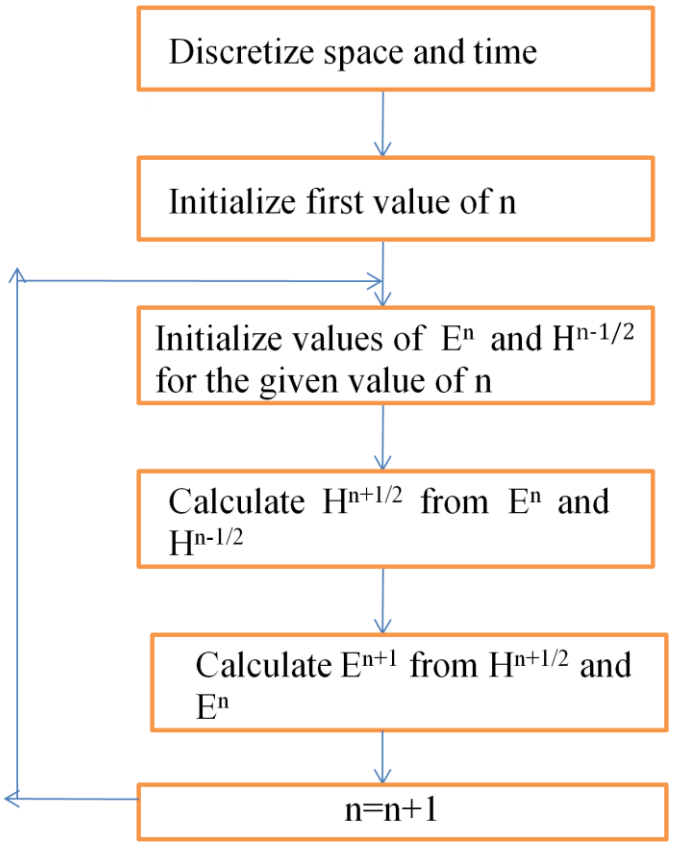

Fig3.5: The FDTD Algorithm

Chapter 4

OPTICAL WAVEGUIDE FILTER DESIGN

USING BAND GAP MAPS

4.1 Radius, Lattice constant and Photonic Band Gap

The objective in this thesis is to design a frequency splitting device, also known as an optical demultiplexer, using a 2D photonic crystal. In simple words, its operation can be described as, with light consisting of two or more frequencies incident on the input port, it is expected that each of the separate frequencies will be output via the different channels, or waveguides in the crystal.

The focus is on building a device that can effectively extract three different wavelengths of light, using a 2D photonic crystal, of a hexagonal lattice structure. Of the two widely used methods of lattice structure- **dielectric rods** in air and holes in dielectric medium- design by using the dielectric rods in air method was opted for.

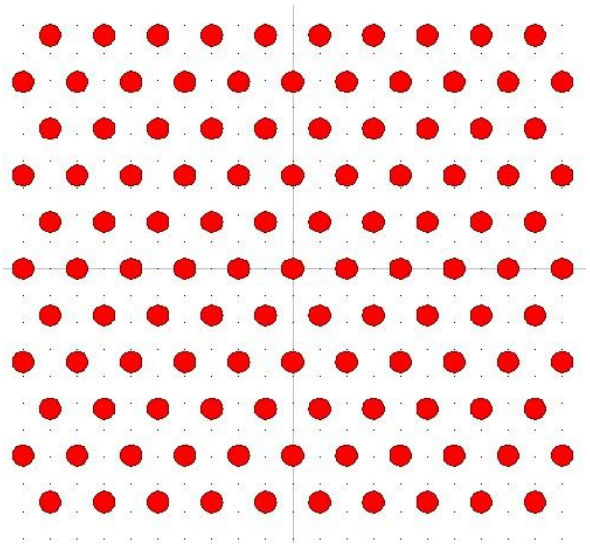

Fig4.1: Lattice structure of the demultiplexer device- the red circles following a hexagonal lattice are the dielectric rods and the white spaces represent air

The **refractive index** of the dielectric medium is arbitrarily chosen to be a value of 3 throughout the whole structure, and that of air is known to be equal to 1. The **radius (r)** and the **lattice constant (a)**-the two key parameters in this thesis- are however not kept constant throughout this lattice intentionally, and it is by the variation of these two properties of the lattice the desired results are obtained.

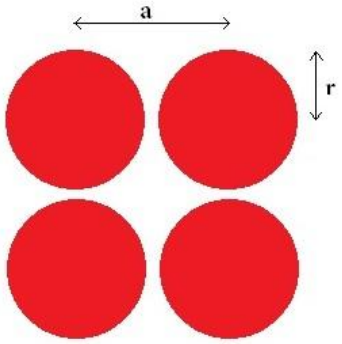

Fig4.2: Rods in air showing the radius (r) and the lattice constant (a)

Photonic crystals exhibit a certain phenomenon, which is by showing **optical band gaps** to certain frequencies of light, and using this unique property of photonic crystals, it is possible to guide the light through the device as desired. This is achieved by introducing line defects.

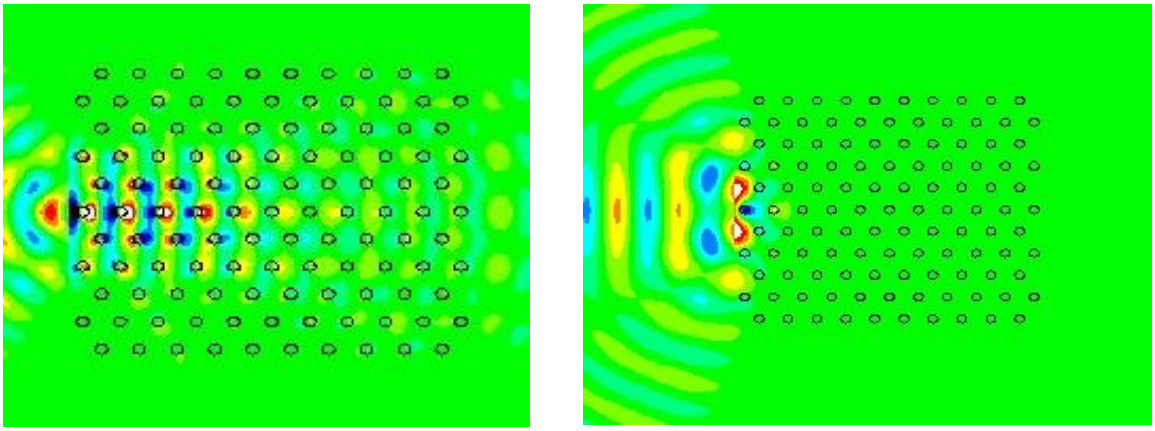

Fig4.3: Photonic crystal showing no band gap to a particular wavelength of light (left) and Photonic crystal showing band gap to a different wavelength of light (right)

To understand which wavelengths will show a band gap on a particular lattice, a **dispersion relation** diagram is consulted. A dispersion relation diagram shows the dependence of the resonant frequencies on the wave vector of the radiation passing through it. (Sukhoivanov, et al. 2009) It is calculated by the **Plane Wave Expansion** (PWE) method and has already been covered earlier.

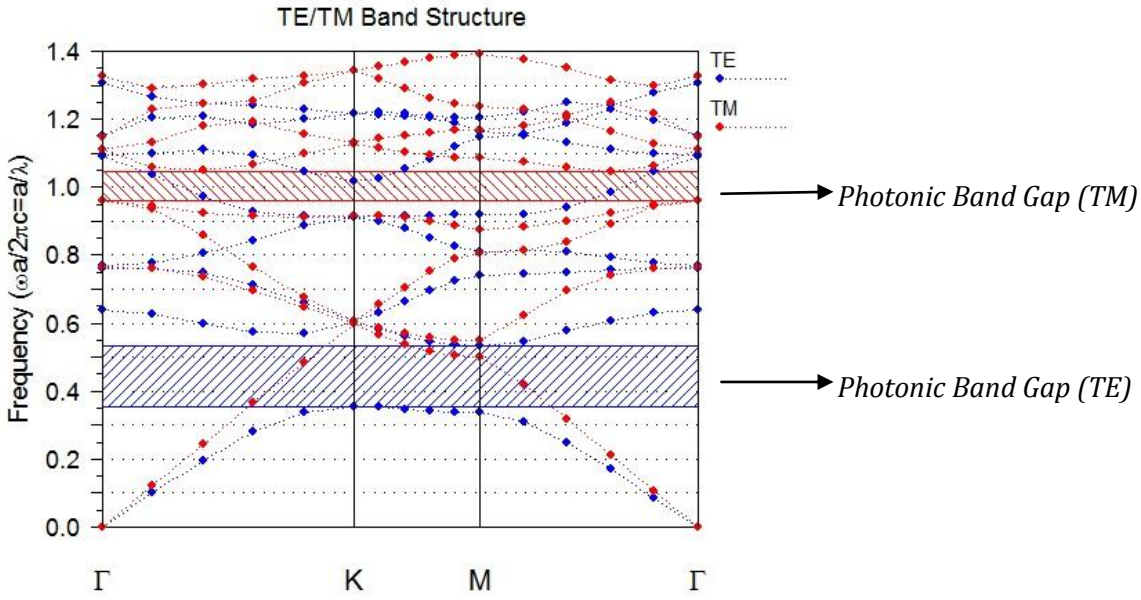

Fig4.4: A sample dispersion relation of a photonic crystal lattice showing the allowed modes and the disallowed modes (band gaps) over the first brillouin zone

It is to be noted that, the dispersion relation is fixed for a particular set of radius and lattice constant values, and if any one of these two properties are altered, the dispersion relation changes. Therefore, a band gap map is plotted, in which the ratio of the radius and lattice constant (r/a) is taken as the independent variable and the allowed and disallowed modes through the chosen lattice is found. The whole calculation involves finding out the dispersion relations at each value of the 'r/a' ratio of a crystal lattice with arbitrary radius and lattice constant, and then plotting them in a single diagram. The CAD software- **RSoft Photonics CAD Suite** is used for this calculation, and all the subsequent calculations (including FDTD) that follow in this thesis.

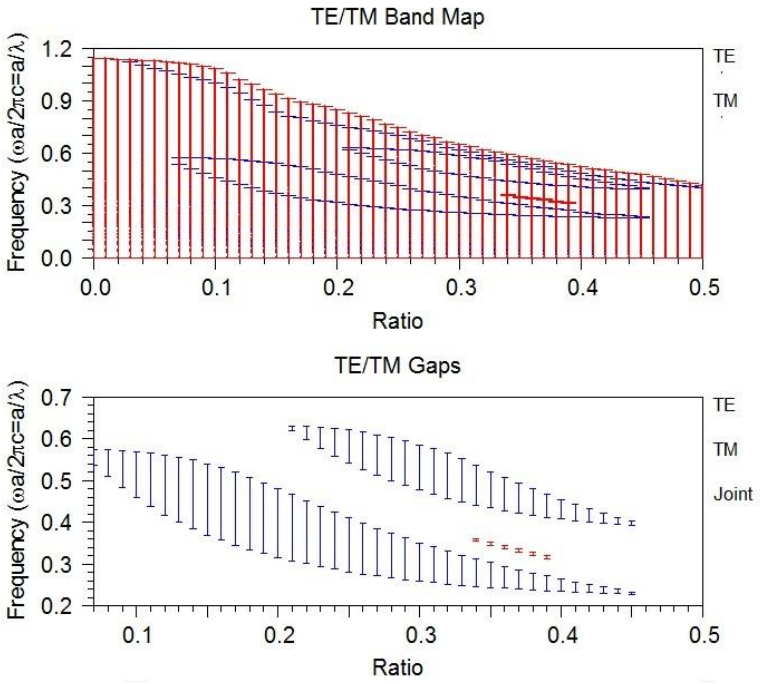

Fig4.5: Figure showing band map with the allowed modes and a gap map below which is formed from the defects in the band map. Both are plotted as normalized frequency against ratio (r/a)

There are primarily, two different polarization modes, the **Transverse Electric** (TE) and the **Transverse Magnetic** (TM) modes. If magnetic component **H** of the plane wave is parallel to the incidence plane, one gets the TE mode. On the other hand, if electric component **E** is parallel to the incidence plane, it leads to a TM mode. (Sukhoivanov, et al. 2009) In this work, the proposed device supports TE modes.

In figure 4.5, a band map is shown and also its corresponding gap map. This shows the photonic crystal's response to a number of wavelengths of light in response to having a number of different 'r/a' ratios. The dispersion relation calculated for each ratio is done by considering the effects of light on only one dielectric rod, known as a **unit cell**. However, in order to obtain a more accurate result, and to replicate the behaviour of the whole crystal lattice, more than one rod is used which are arranged in a periodic manner so as to represent the repetition present in the whole lattice. Figure 4.6 shows this collection of rods that have been used, known as a

supercell. The cells that are coloured green are together used as a supercell for the dispersion relation calculations.

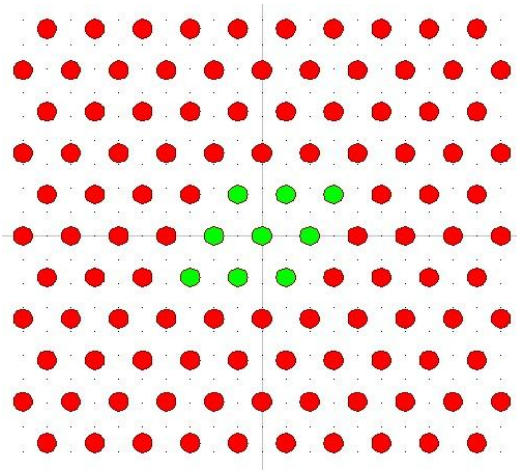

Fig4.6: Supercell within the lattice (coloured in green)

4.2: Optical Waveguide Filter Design

An optical demultiplexer takes as input more than one wavelengths of light, and gives as output each single wavelength via individual channels. A schematic diagram of the design that is followed is shown in figure 4.7.

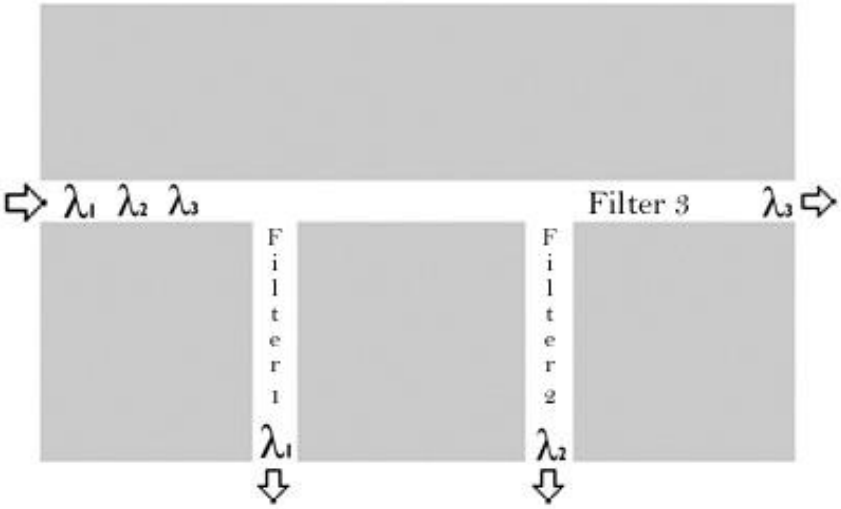

Fig4.7: Schematic diagram of the optical demultiplexer device

For design simplification, and ease of calculation, it was chosen to work with three operating wavelengths of light. They have been decided according to the wavelength regions in the 'telecom windows' used for optical fibre communications. (Dr. Rüdiger Paschotta, Encyclopaedia of laser physics and technology) **1.66 μm**(1660nm), **1.35 μm** (1350nm), and **1.50 μm** (1500nm) are the wavelengths of operation for this device. It is to be understood that,

the purpose of this research is to not only stay limited within these three wavelengths, but to merely formulate a general device structure, whose properties (r/a) can be altered to achieve the same effects from other wavelengths.

It is seen in figure 4.7, that light of three different wavelengths enter the device through the input waveguide (marked with an arrow) and each wavelengths, namely λ1, λ2 and λ3 leave the device through separate channels, from where they may be collected for further use.

The first step in the design of the device is to fix the radius and lattice constant of the dielectric rods to be used in the photonic crystal lattice. The refractive index of the material has already been mentioned earlier to be three (3), set arbitrarily. In order to set the radius and lattice constant, the band gap map proves to be of great help, found earlier from the dispersion relations at different ratio (r/a) values. For greater accuracy, a more precise version of the band gap map shown previously is used. This new band gap map is shown in figure 4.8.

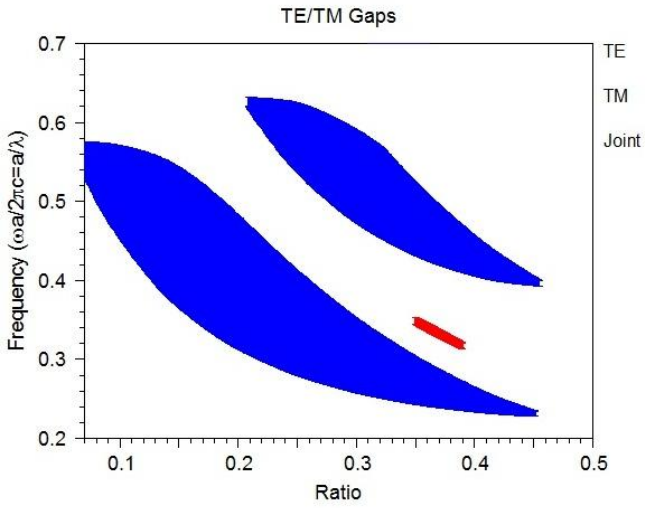

Fig4.8: A more precise band gap map

In figure 4.8, two blue coloured regions signifying the band gap maps of the lattice for the lattice with arbitrary radius and lattice constant for the TE mode is seen. The red region is applicable for the TM mode. Since the device in this thesis is set to work with TE modes only, the red region remains unused.

From the map, the region with the largest gap in normalized frequency is obtained, and the ratio corresponding to the upper and lower normalized frequency values is also obtained, by drawing straight lines as shown in figure 4.9.

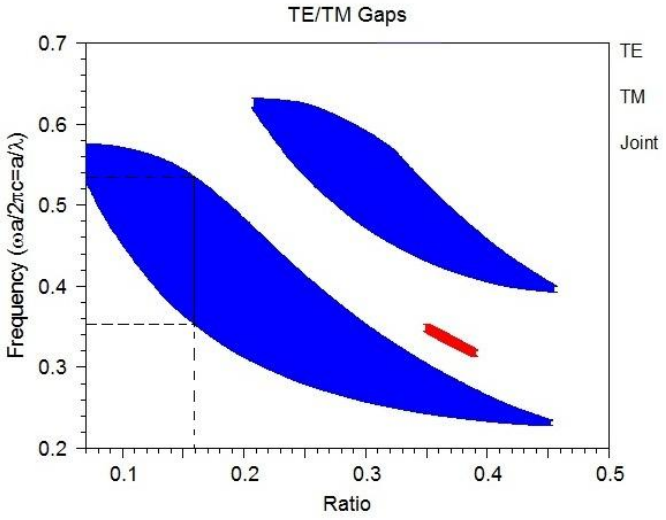

Fig4.9: Band gap map with largest normalized frequency gap identified

The ratio is selected to be roughly 0.16, and the corresponding maximum and minimum values of normalized frequencies are seen to be approximately equal to 0.53 and 0.35 respectively. The operating wavelengths are of a maximum value of 1660 nm and a minimum value of 1350 nm. From this information, a good range for the periodicity or lattice constant values can be calculated, as normalized frequency equals lattice constant over wavelength (frequency= a/λ). It is important that these steps are followed because the aim of the device is to give a band gap to all wavelengths of light falling within 1.66 μm and 1.35 μm so that once inside the defect of the crystal, it will be guided along it by reflecting off the boundaries of the channel that it is in and will not be transmitted out of the crystal unnecessarily.

A range of values for the lattice constant- 0.581<a<0.729 μm is obtained, and one can safely assume a value roughly somewhere in the middle for this design. Thus, a=0.65 μm is decided to be a good value for further calculations. The radius is automatically fixed by the expression defined as- 'Radius=Ratio*Period'- in the software of choice (RSoft Photonics CAD Suite), and with ratio equalling 0.16, a radius value of 0.104 μm is resultant. With these two values (r & a) the lattice of the device is laid out.

The design of the proposed device is desired to be as close to that as possible to the scheme shown earlier. A waveguide allowing all the three wavelengths of light is created by introducing a line defect in the perfectly periodic crystal. Defects are defined as any sort of irregularity introduced in the crystal, and line defects are defined as a series of such consecutive defects taking the shape of a line. In this case, one rod is removed from the crystal and the rod next to it subsequently to create a line defect and form a waveguide. After that, two more waveguides are created in the same way- that are connected to the main waveguide, following the schematic design. Figure 4.10 shows a better picture of this.

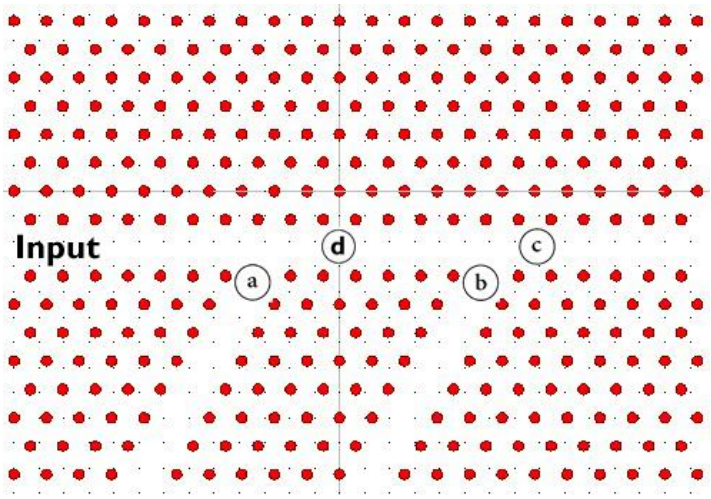

Fig4.10: Photonic crystal lattice showing the three filter waveguides

The letters in circle a, b and c in figure 4.10 indicate the inputs of the three filter waveguides, (a for filter 1, b for filter 2, c for filter 3) where further defects of other sorts are to be introduced in order to filter the incoming light. (The purpose of the label "d" is explained later on in this theis.) For this reason, once again the band gap map is referred (figure 4.9) to obtain specific values of radius and lattice constants of the defects.

In the first filter waveguide, the entrance to which is labelled 'a' in figure 4.10, only the first wavelength is allowed to enter, while the other two of the total three wavelengths are blocked. This is done by placing rods at the entrance of the first filter waveguide, having a ratio of radius over lattice constant fixed by the band gap map. It is assumed that the first wavelength of light has the pre declared value of 1.66 μm. Hence, it is desired to introduce rods which will allow light of wavelength 1.66 μm to pass through it, while showing a band gap to wavelengths 1.35 μm and 1.50 μm. Figure 4.11 shows how an appropriate choice for the ratio from the band gap map is made.

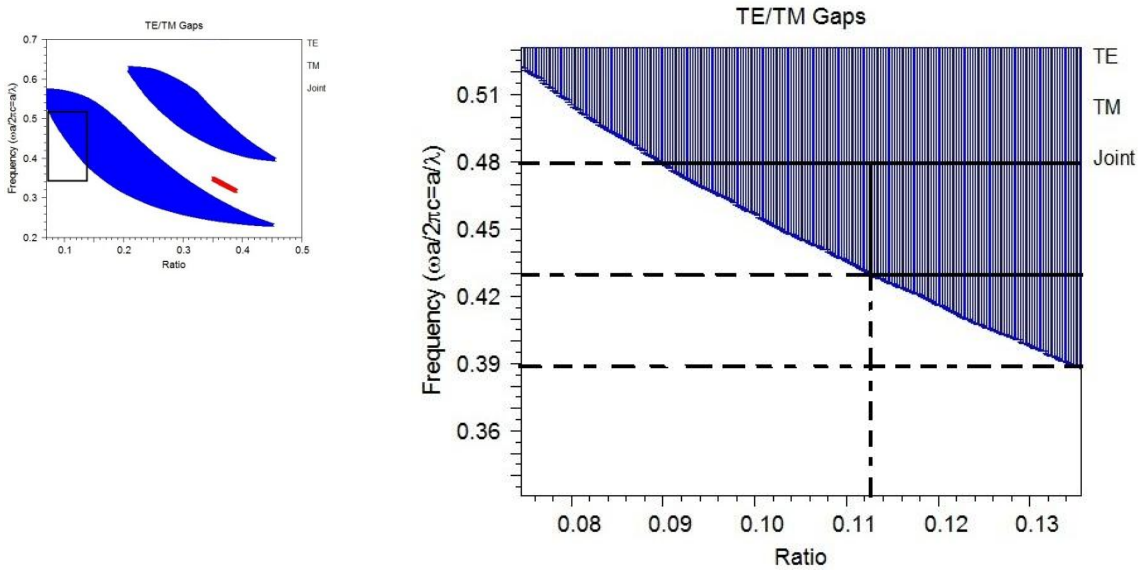

Fig4.11: An enlarged portion of the band gap map (right) and the band gap map showing the area enlarged (left)

Before using the band gap map of figure 4.11, another important concept to understand in this thesis is the use of **normalized frequency** (written as 'frequency' in the y-axis in figure3.11). The normalized frequency is used so that the map is applicable for any scale of lattice used, by the use of a simple relation, "normalized frequency=a/λ". The periodicity of the design lattice is set to be equal to 0.65 μm, which gives the normalized frequencies of the three wavelengths to be used for the design in this thesis as-

For λ1, normalized frequency= 0.65/1.66= 0.3916

For λ2, normalized frequency= 0.65/1.50= 0.4333

For λ3, normalized frequency= 0.65/1.35= 0.4815

From the above information, it will now be more convenient to read off the values from the gap map. In figure 4.11, three horizontal straight lines are drawn corresponding to the frequencies in use. The purpose of the first filter waveguide is to block the frequencies 0.4333 and 0.4815, while allowing only 0.3916 to pass through it. This means that, it is necessary to find a ratio of 'r/a' that puts the two frequencies (0.4333 and 0.4815) inside the blue region of the map, while the remaining frequency to lie outside it. From several possible options, one such ratio value is shown in the figure 4.11, to be approximately equal to 0.113.

Once again, there are two options to work wih. Either to keep the periodicity of the lattice intact in the new defect rods and change the radius only, or to keep the radius equal to all the other rods in the lattice and only change the periodicity. For this thesis, it was chosen to change the radius and keep the periodicity constant for all the defect rods. Figure 4.12 shows the lattice of the device just after the introduction of a new defect rod at point 'a'. The radius of the rod is fixed by the relation (0.65*0.113=) 0.073 μm, and is slightly altered to get an optimal value.

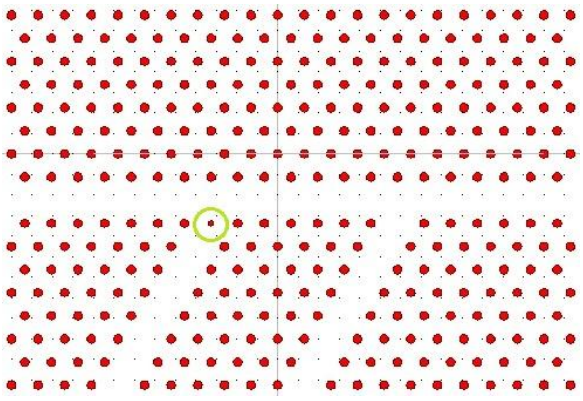

Fig4.12: One defect rod introduced in the first output waveguide entrance (circled in green)

Now, going back to figure 4.10, the label-'d' on the diagram is explained. In order for the demultiplexer device to work properly, it must be ensured that light of only the desired frequency can leave through the channel it is intended to occupy, and not some other wavelength. For example, the light of wavelength 1.66 μm should only be able to exit through the first waveguide labelled 'a', and not 'b' or 'c'. Thus, although the waveguides at 'b' and 'c' would show a band gap to any light of wavelength 1.66 μm that does not follow waveguide 'a', it

would already travel pretty far to be blocked. To ensure that this unwanted light is blocked much closer, for instance, at point “d”, yet another defect is introduced there. The purpose of this new defect rod at “d” will be to exhibit a band gap to the light of wavelength 1.66 μm, while allowing the other two operating wavelengths of light.

Hence, in a fashion similar to the one that was used to find the ratio parameters of the defect rods at ‘a’, the parameters of the defect rods at “d” is found. Figure 4.13 shows how.

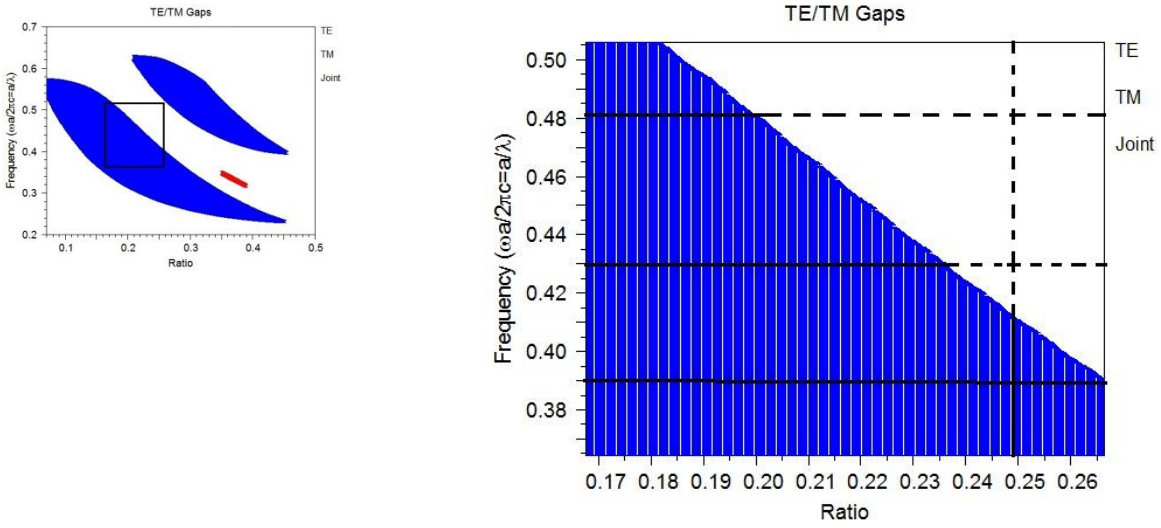

Fig4.13: An enlarged portion of the band gap map (right) and the band gap map showing the area enlarged (left)

From figure 4.13, a suitable ratio (r/a) for the defect rods at “d” to be equal to 0.25 is taken, which makes their radius equal to (0.65*0.25=) 0.1625 μm. Figure 4.14 shows the picture of the lattice after the introduction of dielectric rods at region “d”.

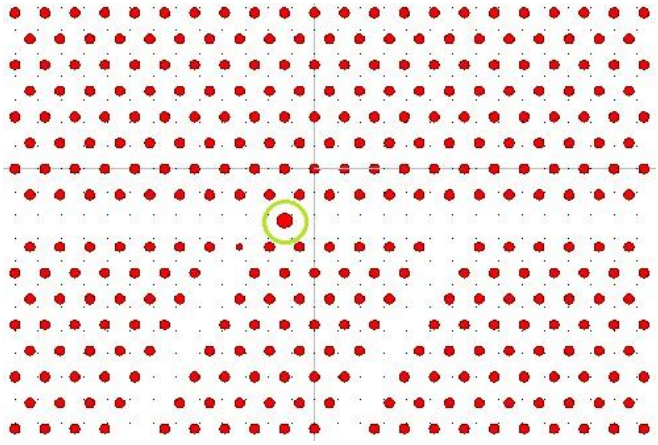

Fig4.14: One defect rod introduced to region “d” (circled green)

The next steps, i.e. finding the appropriate radius over lattice constant value (ratio) for the next two output waveguides labelled “b” and “c” (in figure 4.10) are done exactly the same way as was done for finding the values at regions “a” and “d”. The radius of defect rods at “b” is

found to be (0.09*0.65=) 0.06175 µm, such that it shows a band gap to light of wavelength 1.35 µm, while allowing 1.50 µm. Similarly, the radius of defect rods at "c" is found to be (0.22*0.65=) 0.143 µm, such that it shows a band gap to light of wavelength 1.50 µm, while allowing 1.35 µm. The lattice looks as shown in figure 4.15 after the introduction of the two new defect rods at the remaining waveguide entrances.

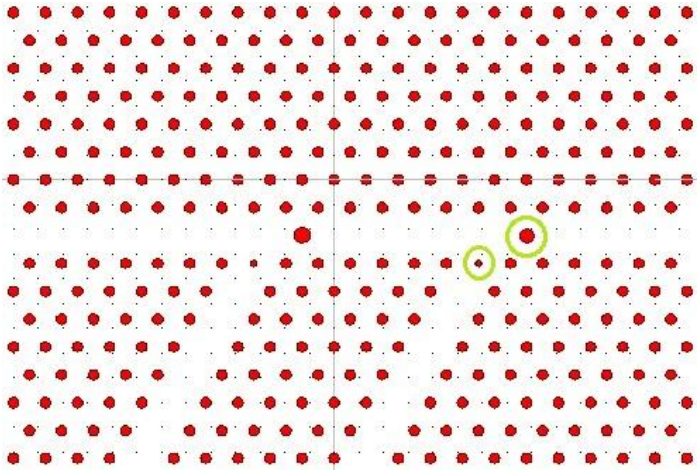

Fig4.15: Lattice after 2 new defect rods introduced

After the layout of the design of the device, it is tested by the help of the FDTD (Finite Difference Time Domain) engine in the software, RSoft Photonics CAD Suite by simulating the propagation of the chosen wavelengths through the waveguides, and observe its behaviour.

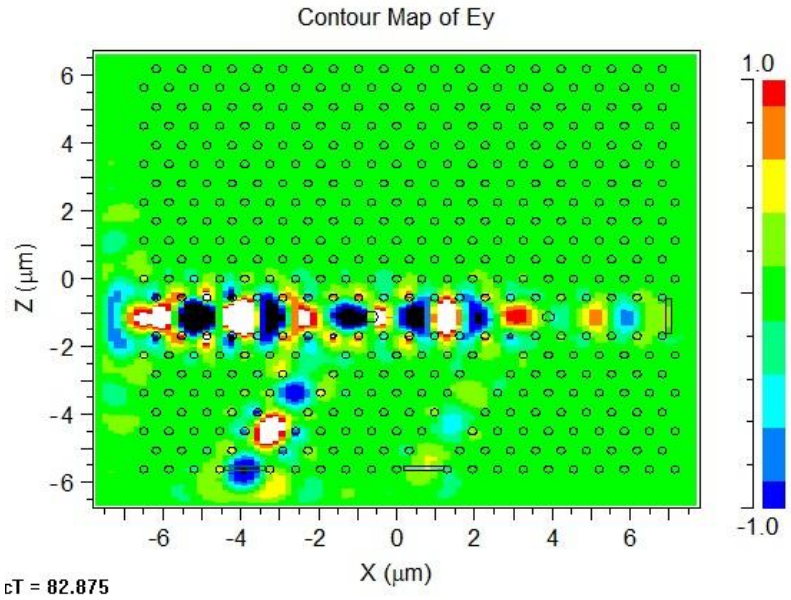

Fig4.16: Screen capture of an FDTD simulation

4.2.1: Response of the device to the light of wavelength 1.66 µm

Figure 4.17 shows a screen capture of the FDTD simulation

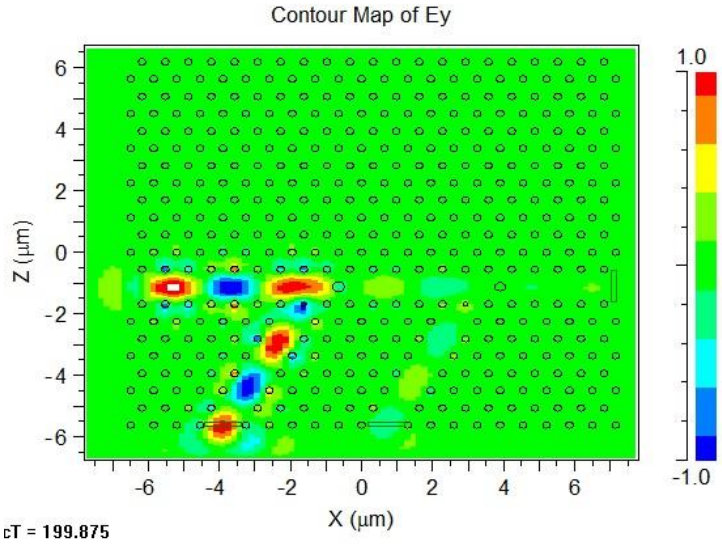

Fig4.17: FDTD simulation showing light of wavelength 1.66 µm propagation

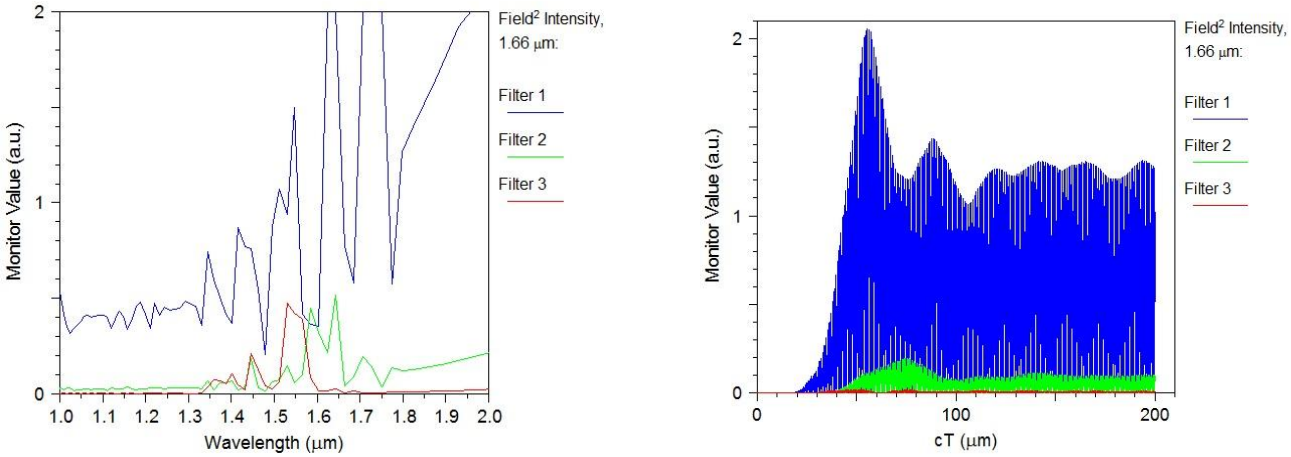

Fig4.18: Wavelength monitor (left-, showing the relative intensities of the lights of different wavelength) and time monitor (right- showing the relative intensities of light at the exit of the filter in real time) corresponding to 1.66 µm

The figures 4.17 and 4.18 represent the results when only light of wavelength 1.66 µm is fed to the device. Although not evident from the screen capture of figure 4.17, a significant portion of light is not being filtered by the filter 1 (as was supposed to), and rather exits the device through other waveguides (filters 2 and 3). This can be seen more clearly from the time monitor of figure 4.18, in which the blue region corresponds to the relative intensity of light seen at the exit of the filter 1. However, the green regions show that intensity of this light is also high at the exit of other filters, which is unwanted. From the wavelength monitor of figure 4.18, (which shows the intensity of the wavelength of light extracted at the ends of the three filter waveguides) it is seen that there is a spike at 1.66 µm in the colour blue (representing filter 1). This signifies that the first filter is working properly. Few tweaks in the design to get a more optimal value are discussed later in this thesis.

4.2.2: Response of the device to the light of wavelength 1.50 µm

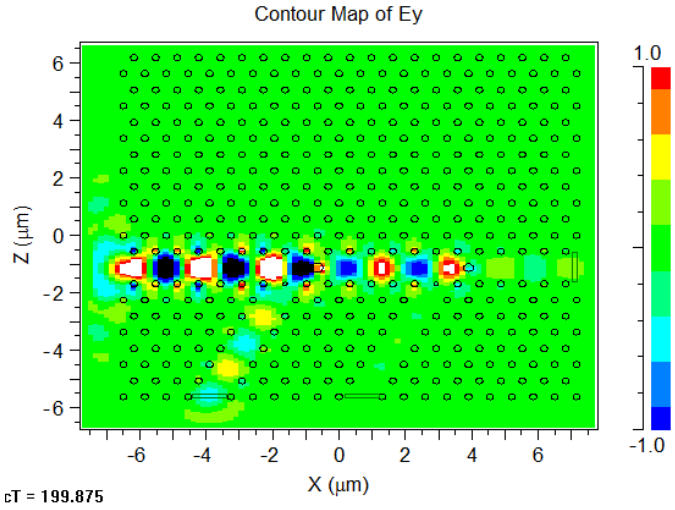

Fig4.19: FDTD simulation showing light of wavelength 1.50 µm propagation

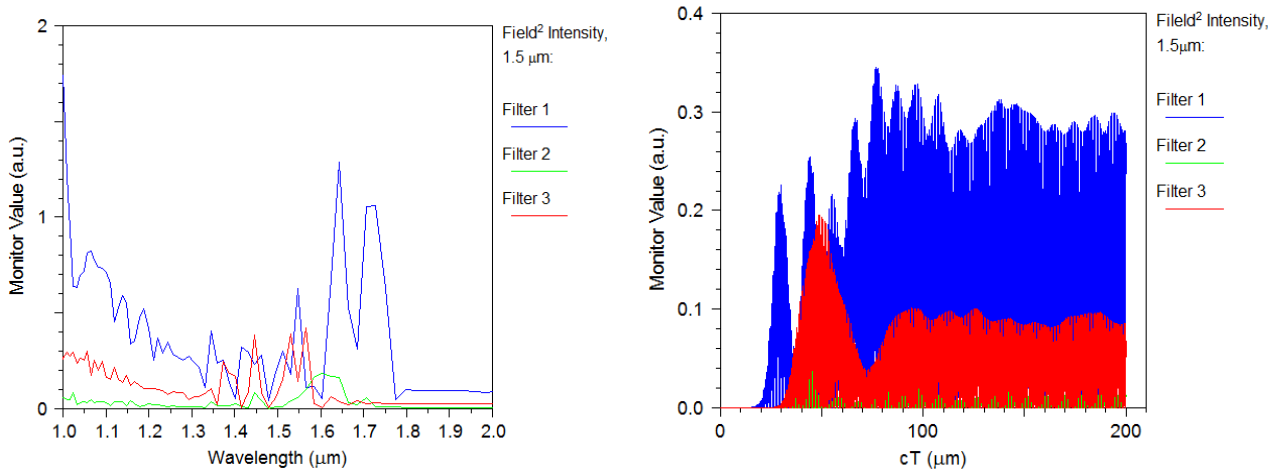

Fig4.20: Wavelength monitor (left-, showing the relative intensities of the lights of different wavelength) and time monitor (right- showing the relative intensities of light at the exit of the filter in real time) corresponding to 1.5 µm

From the figures of 4.19 and 4.20 it is understood that the design for the extraction of the light of wavelength 1.50 µm is not efficient at all, as most of the light is leaked through the first filter waveguide instead of the second, and the intensity of this light at the exit is higher in the first filter waveguide than filter 2, which is absolutely undesirable. A solution to this problem and more optimal results are discussed later in this thesis.

4.2.3: Response of the device to the light of wavelength 1.35 µm

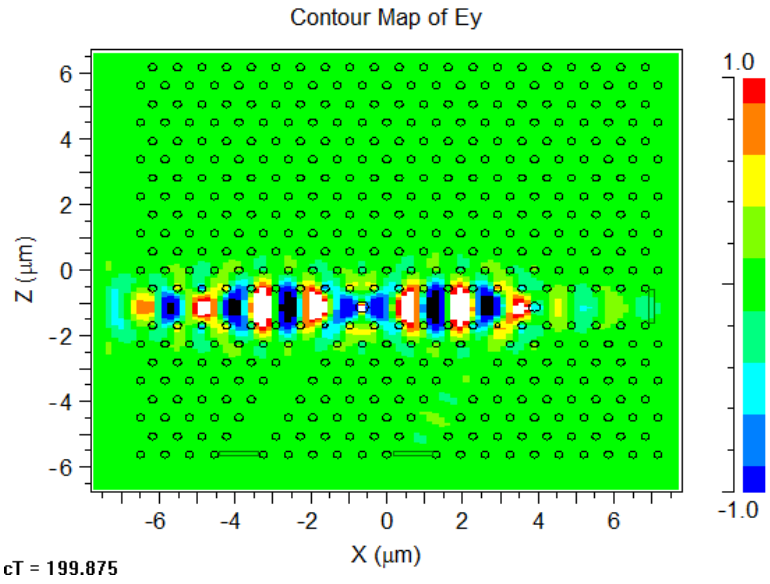

Fig4.21: FDTD simulation showing light of wavelength 1.35 µm propagation

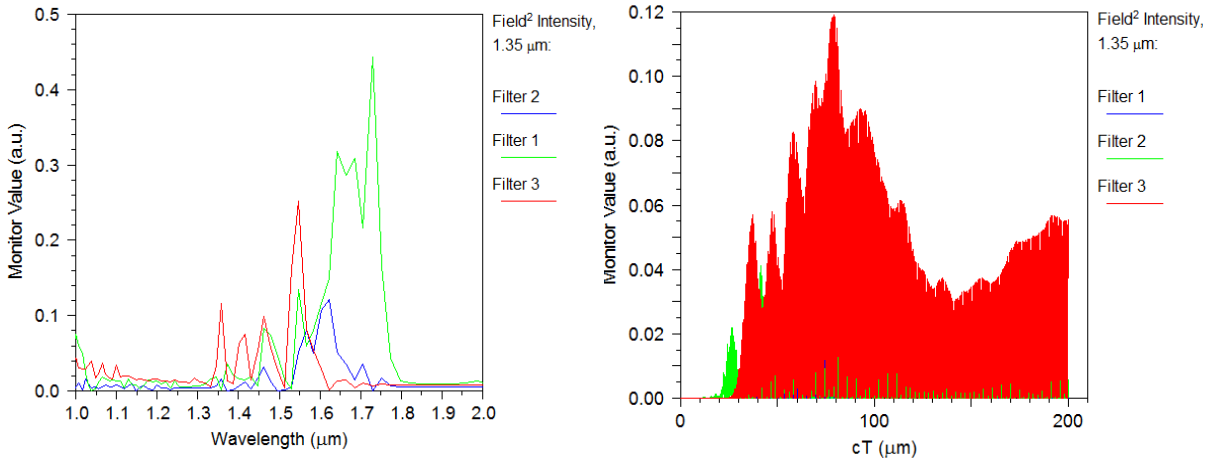

Fig4.22: Wavelength monitor (left-, showing the relative intensities of the lights of different wavelength) and time monitor (right- showing the relative intensities of light at the exit of the filter in real time) corresponding to 1.35 µm

The FDTD simulation's screen capture in figure 4.21 shows that very little of the light of wavelength 1.35 µm actually exits the designated waveguide, i.e. through the filter 3. Although this is better than the FDTD results of the light of wavelength 1.50 µm (looking at the red region of the time monitor of figure 4.22) the wavelength monitor shows otherwise- spikes at wavelengths other than 1.35 µm are higher in intensity than that of 1.35 µm. This calls for better design because of poor efficiency, something that is focused on in the coming parts of this chapter.

4.3: Optimisation of the optical filter

From the preceding pages it was learnt that the design for the filter waveguides have not been up to the standards that are expected of it. An improved design with better efficiency is obtained by the end of the discussion in this part of the current chapter. The problems faced with each wavelengths of light are separately tackled, and solutions for each of them are proposed.

4.3.1: Optimisation of filter 1

It was noticed in section 4.2.1 that compared to the other two wavelengths of light in concern, the 1.66 μm wavelength of light gave a much better result. Hence, any changes to its key parameters (radius and lattice constant) were not done. However, other amendments to get better efficiency by changing the number of dielectric rods at the entrance "a" of the waveguide are addressed from here on. Figure 4.23 shows the relative intensity vs. time plots of the light of wavelength 1.66 μm, obtained from the FDTD simulations for a different number of dielectric rods at "a" each time. The intensity of light is measured at the very end of the filters in each of the subsequent FDTD calculations, so as to get a picture of the output.

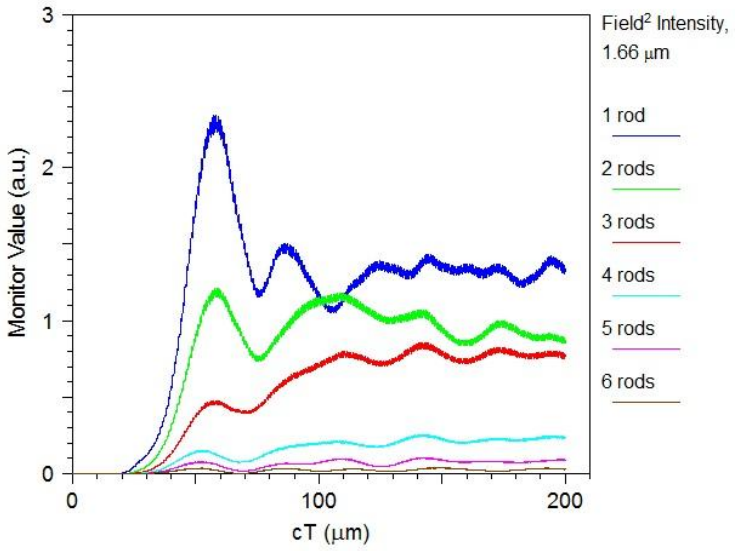

Fig4.23: Filter 1 transmittance intensity of 1.66 μm at different number of dielectric rods

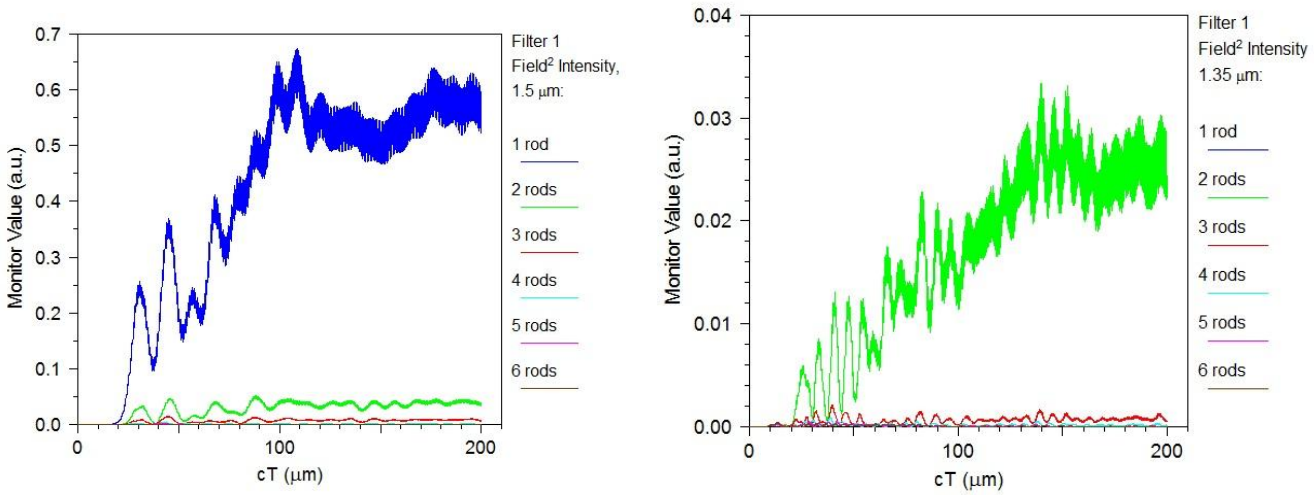

Fig4.24: Filter 1 leakage intensity of 1.5 μm (left) and of 1.35 μm (right) at different number of dielectric rods

From figures 4.23 and 4.24, it is observed that maximum transmittance of the light of wavelength 1.66 μm occurs with only one rod, but at the same time, with just one rod, the leakage of the other two wavelengths 1.35 μm and 1.5 μm are pretty high, which is undesired. Hence, a trade off is opted, going for introducing 3 rods at the entrance of filter 1, which shows a fairly high transmittance to the wavelength 1.66 μm while blocking the other two wavelengths sufficiently well.

4.3.2: Optimisation of the main waveguide leading to filter 2 and 3 (Region "d")

Earlier the use of placing dielectric rods at the region "d" of the lattice structure was discussed and justified. The objective of this waveguide is to only allow light meant for filters 2 and 3, while blocking the light meant to exit through filter 1. Without changing its key parameters, and in a similar fashion that was used in section 4.3.1, the relation of the number of rods in region "d" with intensity of light at the mouth of the filters 2 and 3 is seen. FDTD simulation was used to plot the relative intensity of light against time with a varying number of rods.

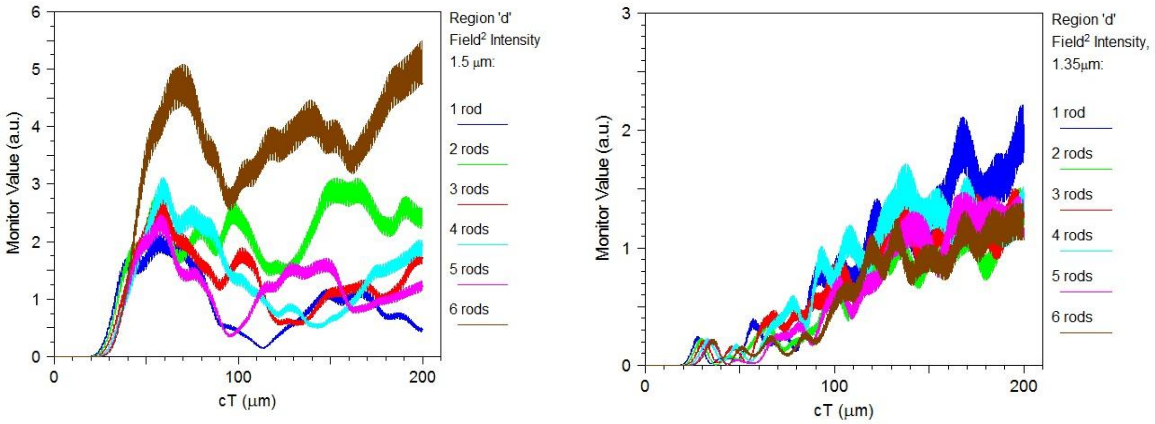

Fig4.25: Region "d" transmittance intensity of 1.5 μm (left) and of 1.35 μm (right) at different number of dielectric rods

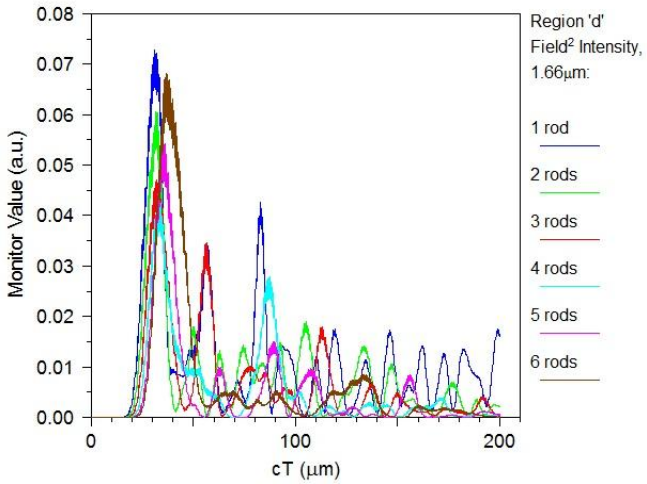

Fig4.26: Region "d" leakage intensity of 1.66 µm at different number of dielectric rods

From the two figures 4.25 and 4.26, it is apparent that a good choice of the number of rods at region "d" would be five rods, as this shows the minimum intensity of light of wavelength 1.66 µm at the entrances of filters 2 and 3, while showing a good response relative to intensity at the same point corresponding to wavelengths 1.35 µm ad 1.5 µm- the two which would be extracted from filters 2 and 3.

4.3.3: Optimisation of Filters 2 and Filter 3

The objective again in the optimisation of filters 2 and 3 is the same as that in the previous two sections- filter 2 would allow the wavelength of light 1.5 µm while blocking 1.35 µm, and similarly filter 3 would allow wavelength of light 1.35 µm while blocking 1.5 µm.

Previously, in section 4.2.2 and 4.2.3, it was found that the responses of both filters 2 and 3 were pretty inefficient compared to that of filter 1. Which is why, in addition to following the optimisation process performed in the preceding two sections, a change in the key parameters of the rods at the entrance of filters 2 and 3 is undertaken. For this purpose, the band gap map in figure 4.8 is again consulted.

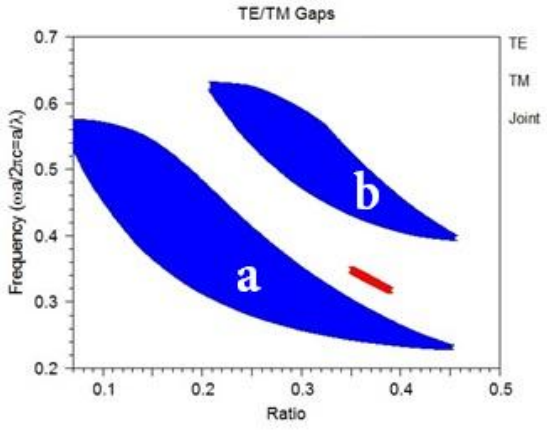

Fig4.27: Band gap maps "a" and "b"

In the previous cases, the use of the band gap map labelled “a” in figure 4.27 was only considered, while in reality, values from band gap map “b” would show the same effects to light as that of “a” and it could very well be used in the determination of appropriate ratio values in the design of filters. As the filters in question, (filters 2 and 3) did not provide a quality output when their defect rods’ radius over lattice constant ratio was determined using band gap map “a”, the band gap map “b” is used in order to get a better coupling.

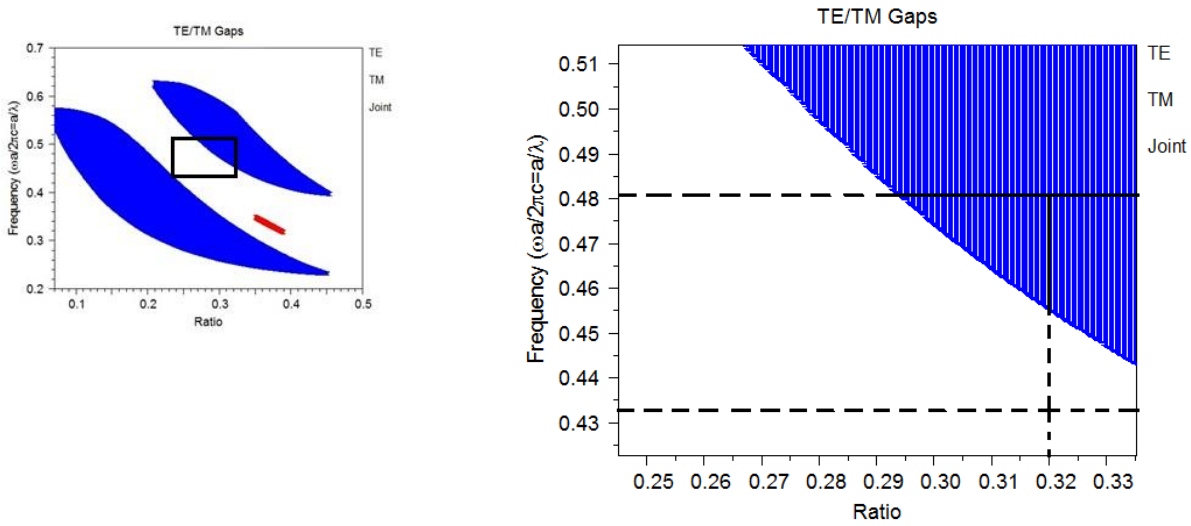

Fig4.28: An enlarged portion of the band gap “b” map (right) and the band gap map showing the area enlarged (left)

The figure 4.28 shows how an appropriate ratio value for filter 2 is found from the band gap map. At about a ratio (r/a) of 0.32 (giving a radius value of 0.208 μm), the normalized frequency 0.48 (1.35 μm) is shown a band gap, i.e. not allowed by filter 2, while allowing the light of normalized frequency 0.433 (1.50 μm). The number of rods with ratio equal to 0.32 to be introduced at the entrance of filter 2 is found in the same way as was done for filter 1. Figure 4.29 shows the FDTD results of the intensity of light at the very end of filter 2 at various numbers of dielectric rods, corresponding to the three operating wavelengths.

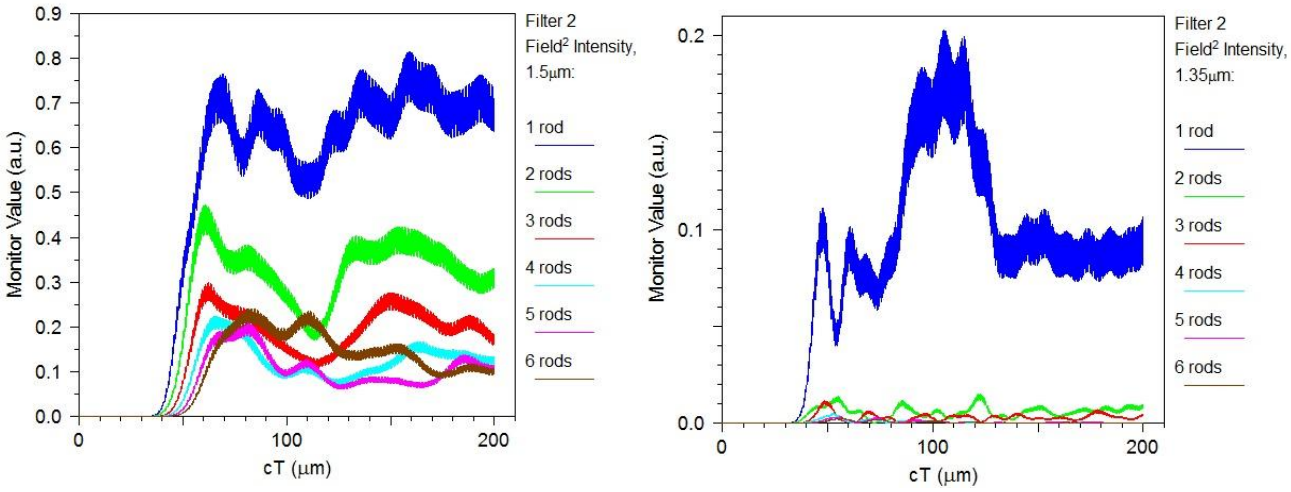

Fig4.29: Filter 2 transmittance intensity of 1.5 μm (left) and leakage intensity of 1.35 μm (right) at different number of dielectric rods

From figure 4.29 it is evident that a choice of 2 rods to be placed at the entrance of filter 2 would be the most efficient option in regards to a good transmission intensity of the desired wavelength (1.5 μm), as well as very little leakage intensity for the undesired wavelength (1.35 μm).

Next an appropriate ratio of radius over lattice constant for the dielectric rods to be placed at the entrance of filter 3 is set. The help of the band gap map "b" was sought once again.

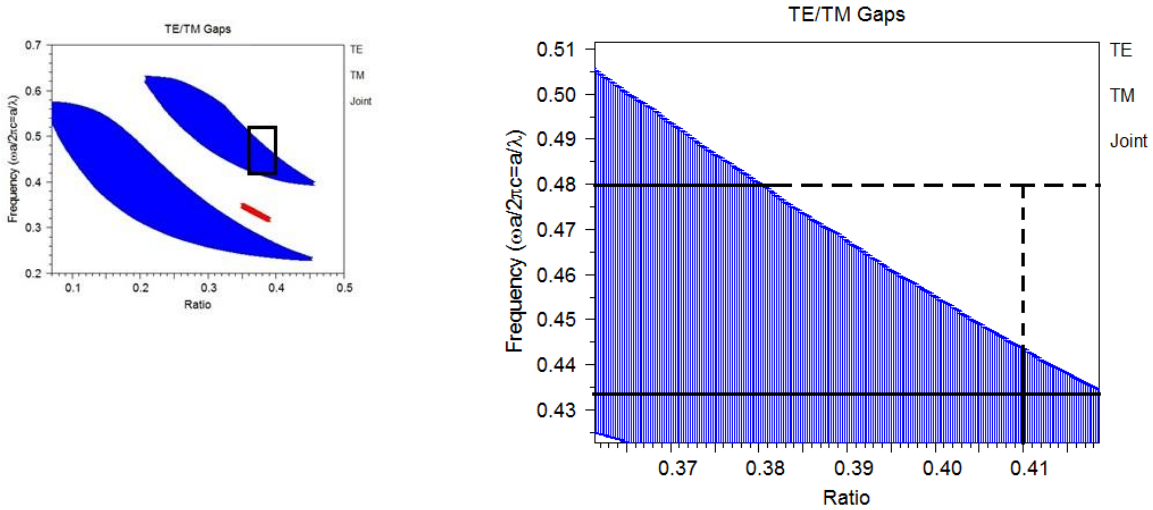

Fig4.30: An enlarged portion of the band gap "b" map (right) and the band gap map showing the area enlarged (left)

The ratio of the rods at filter 3 is determined by the help of figure 4.30, and set to be equal to 0.41 (giving a radius value of 0.2665 μm). At this value, the normalized frequency of 0.433 (1.50 μm) sees a block at filter 3, while 0.48 (1.35 μm) is allowed to enter through it. The number of rods at filter 3 to be placed is found by a comparison of the transmitted (desired) wavelength's intensity and the leakage (undesired) wavelength's intensity at the exit of the filter 3. This is done by various plots of intensity vs. time at different combination of number of rods at filter 3 using FDTD simulations.

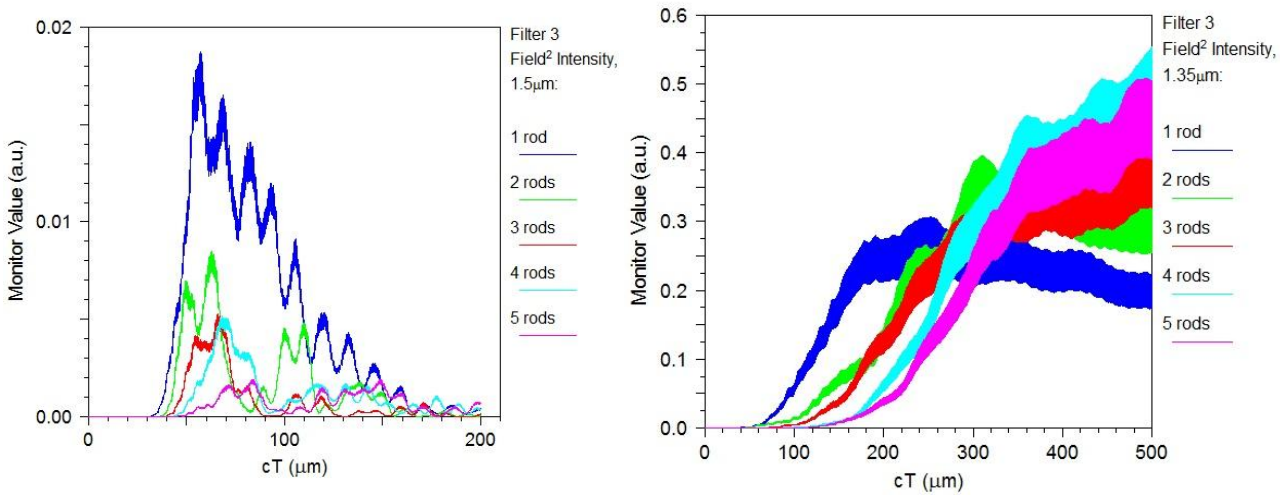

Fig4.31: Filter 3 leakage intensity of 1.5 μm (left) and transmittance intensity of 1.35 μm (right) at different number of dielectric rods

The diagrams in figure 4.24 help decide to put 4 dielectric rods at the entry of filter 3, as it has the greatest transmittance intensity for the light of wavelength 1.35 μm and a fairly low leakage intensity of the light of wavelength 1.50 μm.

After the correct placement of all the rods at the entrance of each filter, the lattice looks as shown in figure 4.32, which is the final view of the three wavelength filter design.

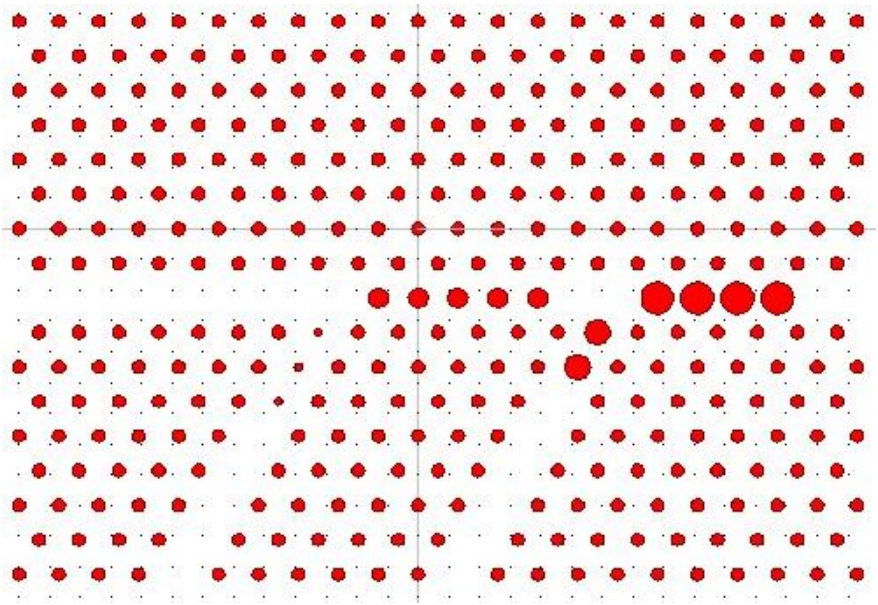

Fig4.32: Lattice structure of the three wavelength filter

Following (figure 4.33) are the screen captures of the FDTD simulation of the device working at each wavelength.

(a)

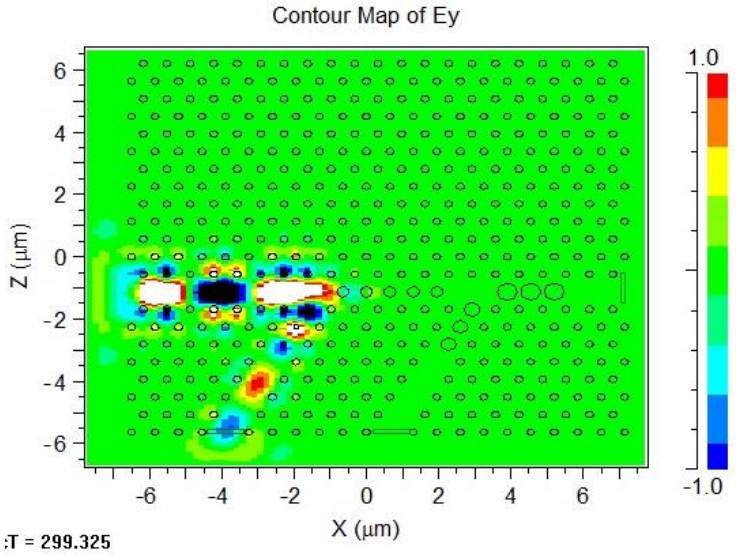

(b)

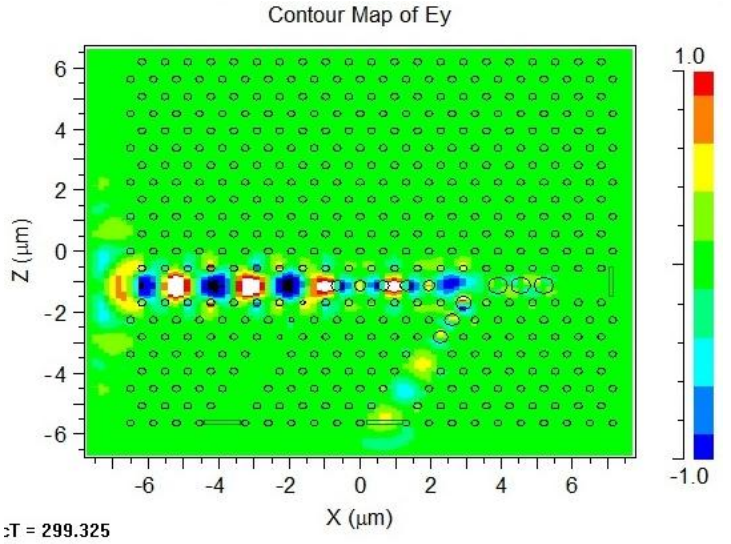

(c)

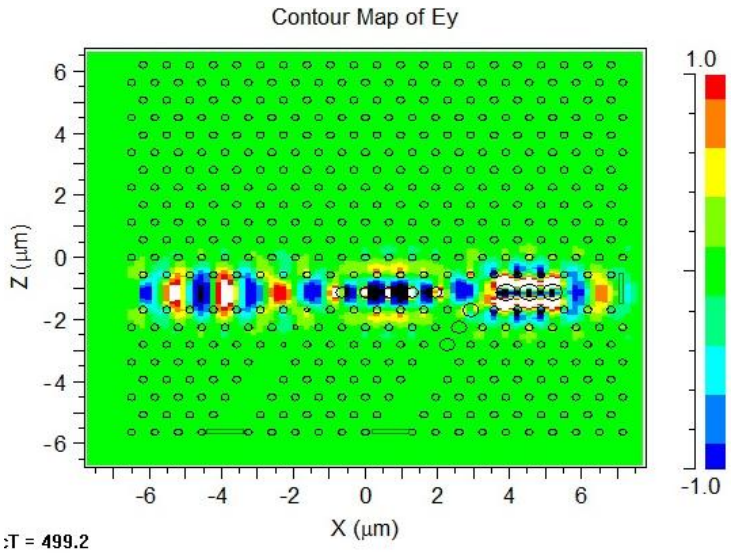

(d)

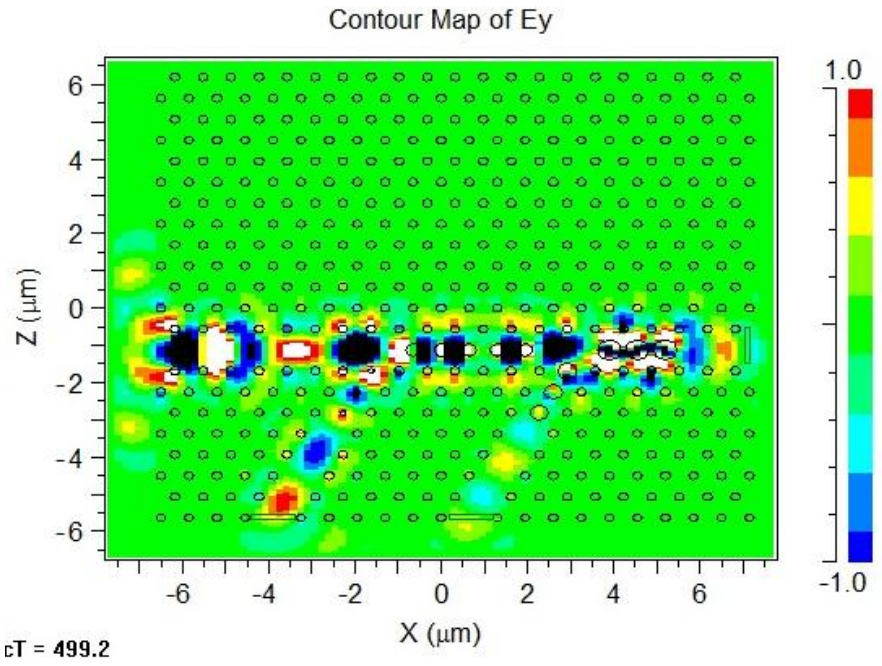

Fig3.33: Filter 1 (a), filter 2 (b) and filter 3 (c) in operation with wavelengths 1.66 μm, 1.50 μm and 1.35 μm respectively; (d) shows the operation of the three filters together

The wavelength response of the three filters is an important finding in this thesis, as it deals with filters. Figure 4.34 shows the wavelength monitors.

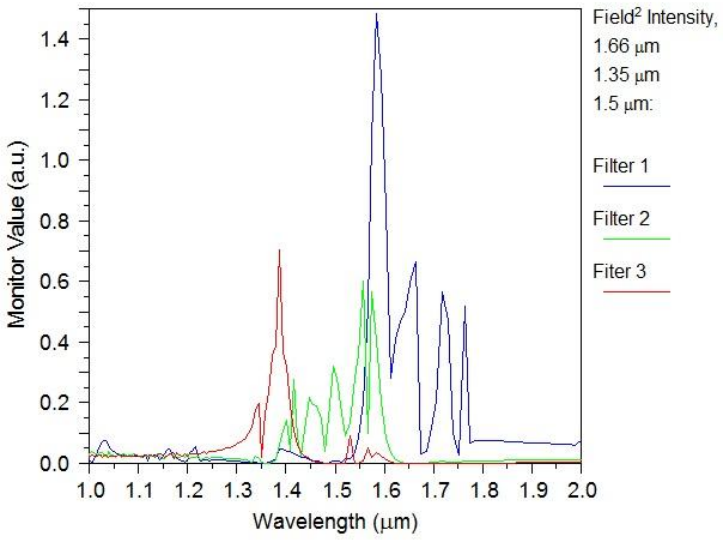

Fig4.34: Wavelength response of the filters

In figure 3.34, it is noticed that instead of giving a sharp rise at one discrete wavelength, the filters show good relative intensities at around the working wavelengths, which is perfectly normal. Thus the red spike around 1.35 μm, the green spikes around 1.5 μm and the blue spikes around 1.66 μm all show that the filters are working perfectly fine and much better with the optimisation performed on it. The slight shifts in wavelength may be due to the fact that the wavelength of light changes inside a dielectric medium. All the wavelengths used for the calculations had been considered to be in free space.

Chapter 5:

CONCLUSION

&

FUTURE RESEARCH

This thesis presents a novel design of an optical filter based on a 2D photonic crystal, by the proper application of the band gap map to tailor the dimensions inside the crystal in order to achieve desired results. The successful separation of three different wavelengths of light, chosen not arbitrarily but in accordance with the actual wavelengths used in the real world fibre optic communication was shown in this research. The findings show that by making appropriate changes to the radius and lattice constant dimensions of the defects introduced in a perfectly periodic PhC (Photonic Crystal), one can filter light of any desired wavelength from a collection of wavelengths, provided it agrees with the band gap map. The proposed design is indeed practical, as it involves the use of only a single base dielectric material in its lattice, with no change in periodicity even in case of the defects- which is definitely an upper hand in case of fabrication.

Some scope for improvement is seen in the proposed design. At some resonant frequencies, relative intensities show off the chart values, while in other cases, they are surprisingly poor- even though the defects were set using the band gap map. This is a peculiar exhibition of the photonic crystals in general, and can be tackled by improving the coupling. In this thesis, it was done by changes in the number of dielectric rods. To investigate the further improvement of the efficiency of the light extracted at the output of the filters, methods other than changing the number of defect rods can be undertaken.

Several WDM (Wavelength Division Multiplexer) components of PhC based demultiplexers have been proposed using various concepts such as resonance, self imaging effect, etc in various research works. [9-14] Whereas the design proposed in this thesis is extensively dependent upon the band gap map analysis, which is simpler to derive. The design of this three wavelength filter also resembles that of a triplexer, an important component in the WDM which plays a key role in the system of FTTH (Fiber to the Home) networks.[15,16] In the near future, with widespread use of the new and much faster type of optical fibre based on photonic crystals, the use of PhC filters would proliferate, and the design in this thesis would act as a great foundation for further research on this topic, as such filters have been widely accepted to be able achieve multiplication in communication capacity by the splitting of the light of multiple wavelengths. Another great scope of further research on the proposed design in this thesis is to achieve a desirable delay in propagation. With that, full-fledged optical processors might even take over their electronic counterparts in the near future.

References:

1. K. Olukotun, L. Hammond, Multiprocessors,3(7) (2005).
2. S. F. Mingaleev, Y. S. Kivshar, J. Opt. Soc. Am. B,19(9), 2241 (2002).
3. S. Noda, M. Imada, M. Okano, S. Ogawa, M. Mochizuki, A. Chutinan, IEEE Journal of Quantum Electronics 38(7), 915 (2002)
4. C. M. Soukoulis, ed., *Photonic Crystals and Light Localization in the 21st Century* (Kluwer, Dortrecht, 2001).
5. John D. Joannopoulos, Steven G. Johnson, Joshua N. Winn, and Robert D. Meade, Photonic Crystals: Molding the Flow of Light second edition, Princeton University Press 2008.
6. M. Bayindir, B. Temelkuran, and E. Ozbay, "Propagation of photons by hopping: A waveguiding mechanism through localized coupled-cavities in three-dimensional photonic crystals," Phys. Rev.B 61, R11855–R11858 (2000).
7. O. Painter, R. K. Lee, A. Scherer, A. Yariv, J. D. O'Brien, P. D. Dapkus, and I. Kim, "Two dimensional photonic band-gap defect mode laser," Science 284, 1819–1821 (1999)
8. J. C. Knight, J. Broeng, T. A. Birks, and P. S. J. Russell, "Photonic band gap guidance in optical fibers," Science 282, 1476–1479 (1998).
9. Niemi, T., Frandsen, L. H., Hede, K. K., Harpøth, A., Borel, P. I. and Kristensen, M. "Wavelength-division demultiplexing using photonic crystal waveguides," IEEE Photon. Technol. Lett. 18(1), 226-228 (2006).
10. Chien, F. S. S., Hsu, Y. J. and Hsieh, W. F., "Dual wavelength demultiplexing by coupling and decoupling of photonic crystal waveguides," Opt. Express 12(6), 1119-1125 (2004).
11. Koshiba, M., "Wavelength division multiplexing and demultiplexing with photonic crystal waveguide couplers," J.Lightwave Technol. 19(12), 1970- (2001).
12. Sharkawy, A., Shi, S. and Prather, D. W., "Multichannel wavelength division multiplexing with photonic crystals,"Appl. Opt. 40(14), 2247-2252 (2001).
13. Kim, H. J., Park, I., B, H. O., Park, S. G., Lee, E. H. and Lee, S. G., "Self-imaging phenomena in multi-mode photonic crystal line-defect waveguides: application to wavelength de-multiplexing," Opt. Express 12(23),5625-5633 (2004).
14. Shi, Y., Dai, D. and He, S., "Novel ultracompact triplexer based on photonic crystal waveguides," IEEE Photon.Technol. Lett. 18(21), 2293-2295 (2006).
15. Shih, T. T., Wu, Y. D. and Lee, J. J., "Proposal for compact optical triplexer filter using 2-D photonic crystals,"IEEE Photon. Technol. Lett. 21(1), 18-20 (2009).
16. http://www.rp-photonics.com/optical_fiber_communications.html, Dr. Rüdiger Paschotta (Encyclopaedia of laser physics and technology).

17. Sukhoivanov, Igor A., Guryev, Igor V., ‘Photonic Crystals- Physics and Practical Modeling’, Springer Berlin Heidelberg, 2009.
18. John D. Joannopoulos, Steven G. Johnson, Joshua N. Winn, and Robert D. Meade, Photonic Crystals: Molding the Flow of Light second edition, Princeton University Press 2008.
19. Meade, R. D., A. M. Rappe, K. D. Brommer, J. D. Joannopoulos, O. L. Alerhand, Accurate Theoretical Analysis of Photonic Band-Gap Materials, Physical Review,1993
20. Frankel, Theodore, The Geometry of Physics, Cambridge University Press 2004.
21. Lipschutz, Seymour, Schaum's outline of theory and problems of linear algebra, Schaum's outline series McGraw-Hill, 1991.
22. S.O. Kasap, ‘Optoelectronics and Photonics-Principles and Practices’, Prentice Hall, 2001.
23. K. Sakoda, *Optical Properties of Photonic Crystals (First Edition)*. (Springer,Heidelberg, 2001).